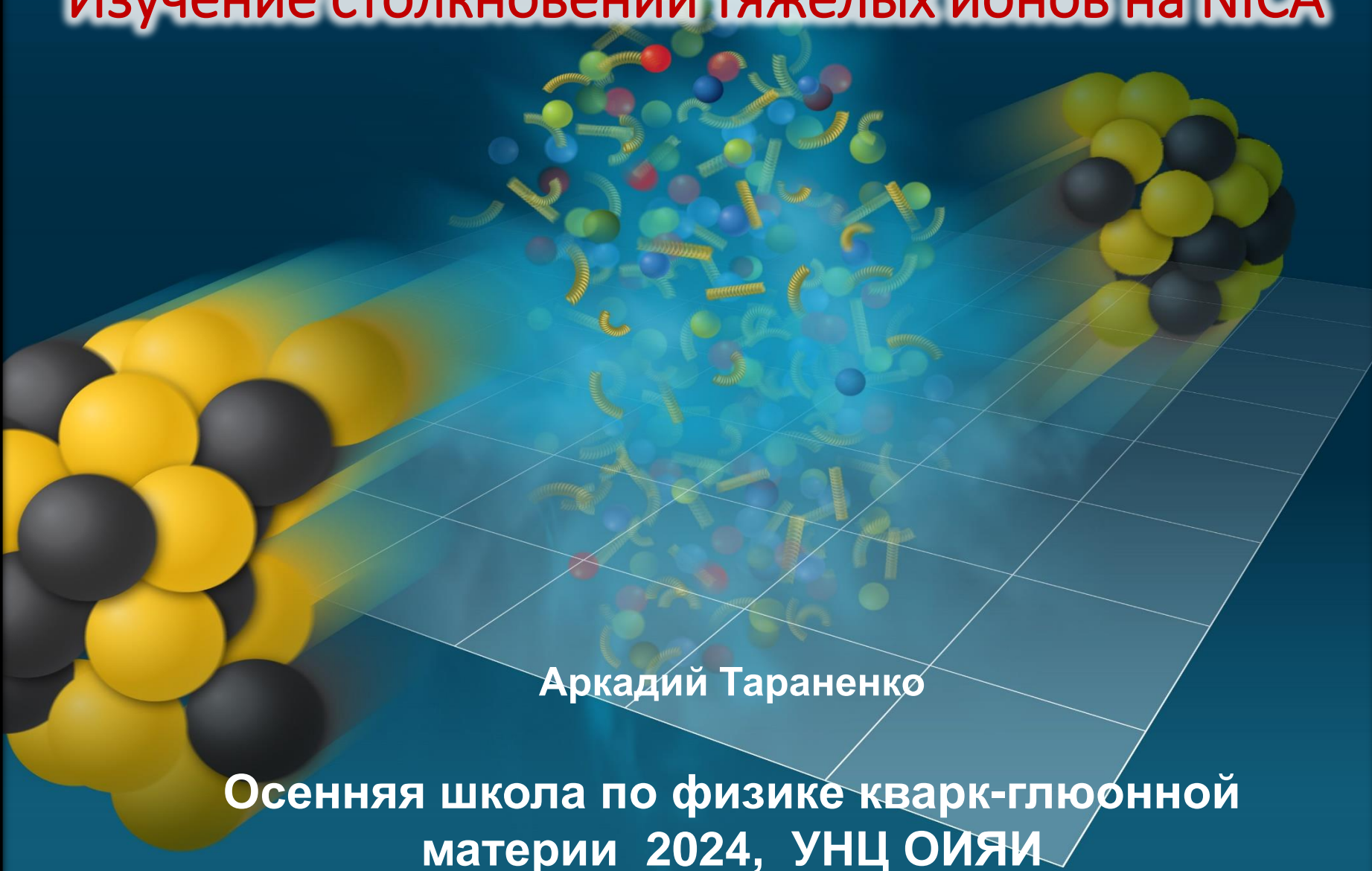


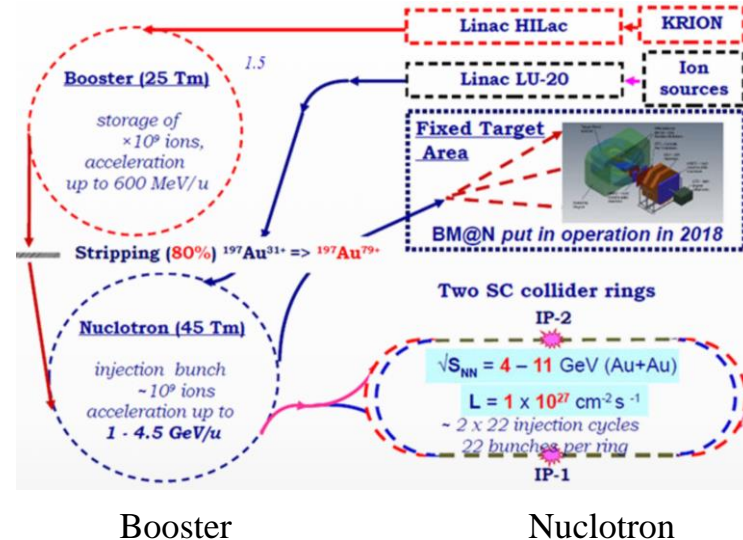
Изучение столкновений тяжелых ионов на NICA



Аркадий Тараненко

Осенняя школа по физике кварк-глюонной
материи 2024, УНЦ ОИЯИ

Ускорительный комплекс NICA (ЛФВЭ, ОИЯИ, Дубна)

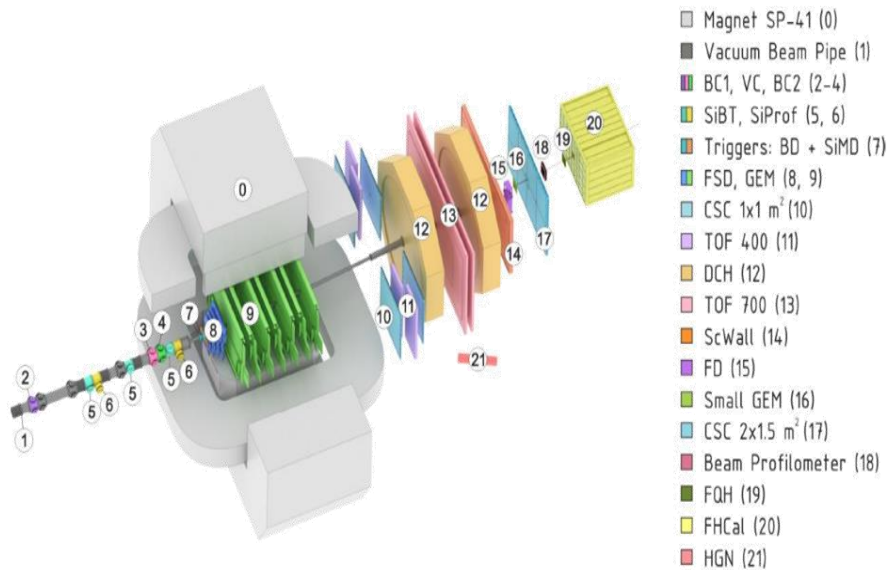


- Мегапроект NICA (Nuclotron based Ion Collider fAcility) - сверхпроводящий коллайдер протонов и тяжёлых ионов, строящийся на базе Лаборатории физики высоких энергий (ЛФВЭ, ОИЯИ), окончание строительства: 2025
 - BM@N (“Барионная материя на Нуклоне”) – Nuclotron, с 2018 года
 - MPD (“Многоцелевой Детектор”) - коллайдер NICA, 2025-2026 год
 - SPD (“Детектор Спиновой Физики”) - коллайдер NICA, 2028-2030 год?

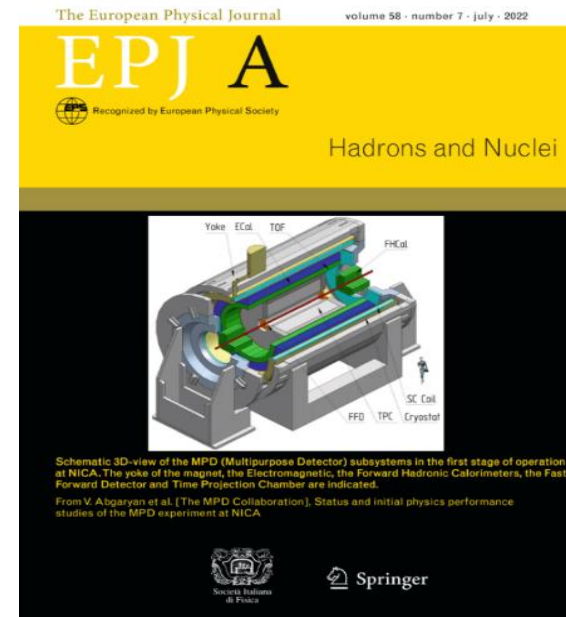
NICA: BM@N and MPD Collaborations

The BM@N spectrometer at the NICA accelerator complex

Nucl.Instrum.Meth.A 1965 (2024) 169352



Status and initial physics performance studies of the MPD experiment at NICA , Eur.Phys.J.A 58 (2022) 7, 140



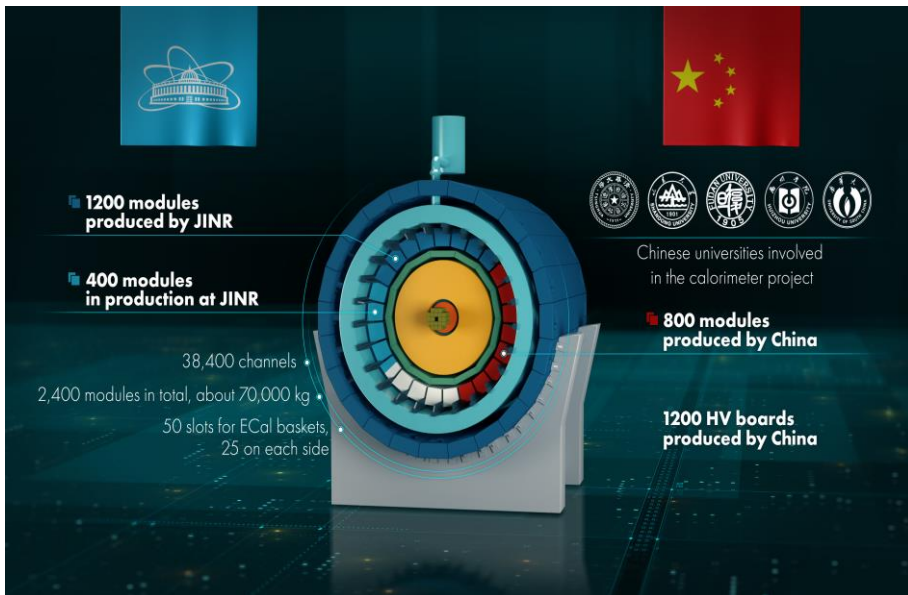
BM@N: ~214 participants из 13 institutes, 5 countries



MPD: ~500 participants из 38 institutes, 12 countries



MPD collaboration (NICA)



The 2nd China-Russia Joint Workshop on NICA Facility
Qingdao, China 2024.9.9–9.12

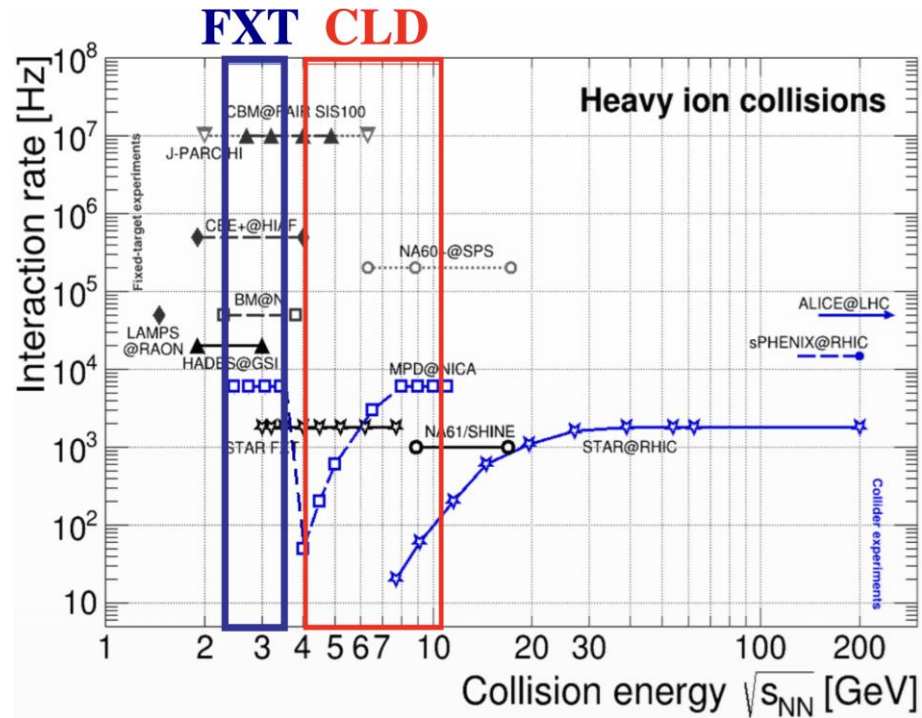
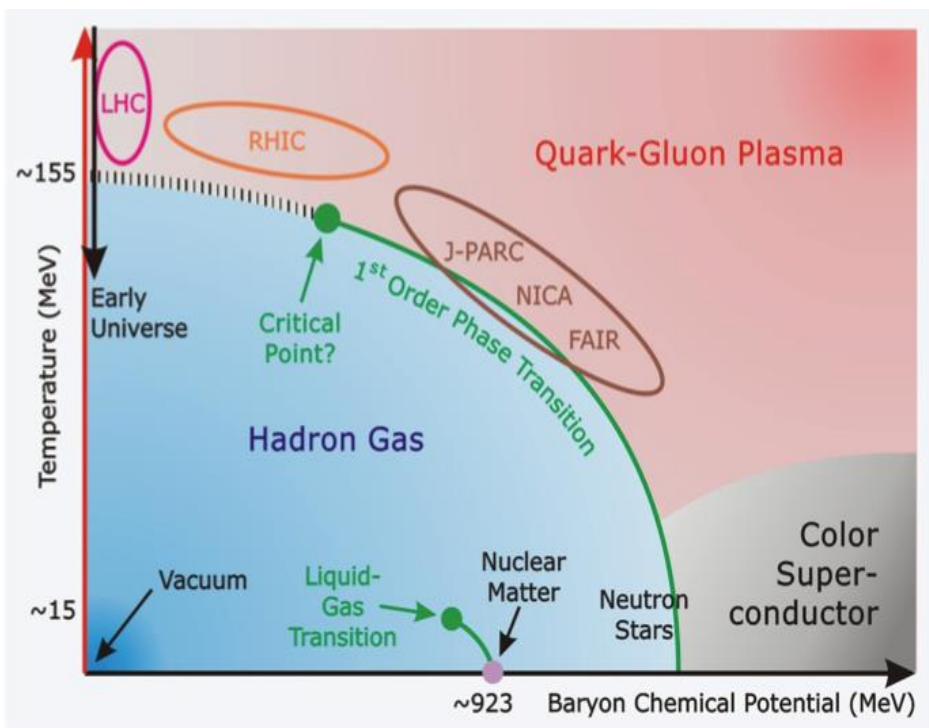


2nd China-Russia Joint Workshop
on NICA Facility
indico.jinr.ru/event/4642

❖ International Workshop on physics performance studies at NICA-2024
(November 25-27, 2024)

<https://indico.jinr.ru/event/4973/overview>





Эксперименты BM@N ($\sqrt{s_{NN}}=2.3\text{--}3.3$ ГэВ) и MPD ($\sqrt{s_{NN}}=4\text{--}11$ ГэВ) будут изучать свойства сильно взаимодействующей материи в области максимальной барионной плотности: столкновения релятивистских ядер.

Доступные источники: C (A=12), N (A=14), Ar (A=40), Fe (A=56), Kr (A=78-86), Xe (A=124-134), Bi (A=209).

Phase transition in Lattice QCD

$$T_c \approx 156 \pm 9 \text{ MeV}$$

[PRD 90 094503 (2014)]

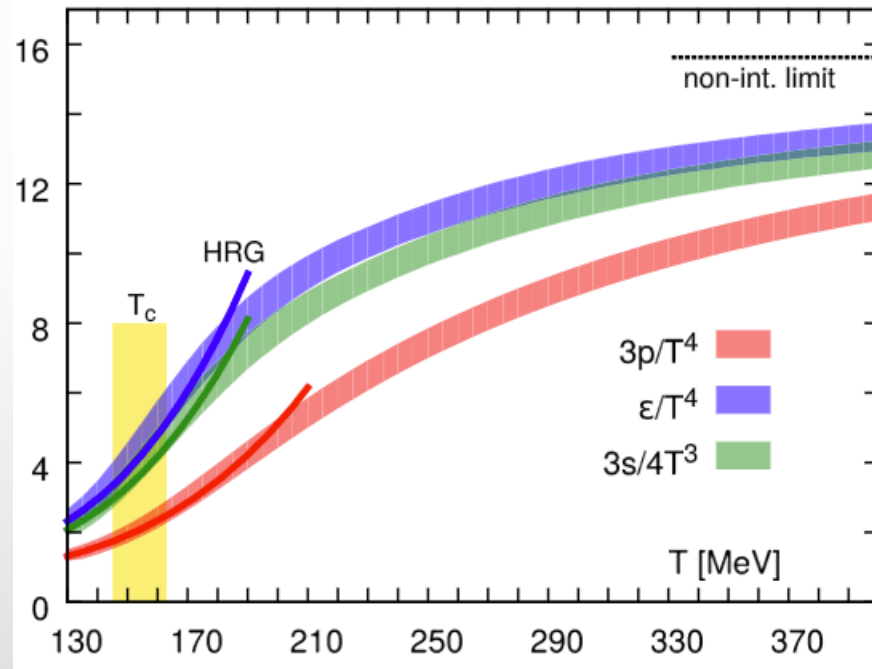
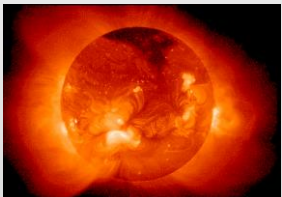
Energy density ε
Pressure p
Entropy density s

For comparison:

$T = 156 \text{ MeV} \approx 1.8 \cdot 10^{12} \text{ K}$

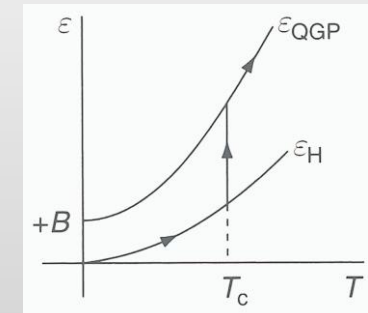
Sun core: $1.5 \cdot 10^7 \text{ K}$

Sun surface: 5778 K



Steep rise in thermodynamic quantities due to change in number of degrees of freedom → phase transition from **hadronic to partonic** degrees of freedom.

Smooth *crossover* for a system with net-baryon content equal 0. For a *first order phase transition*, the behavior would be not continuous.



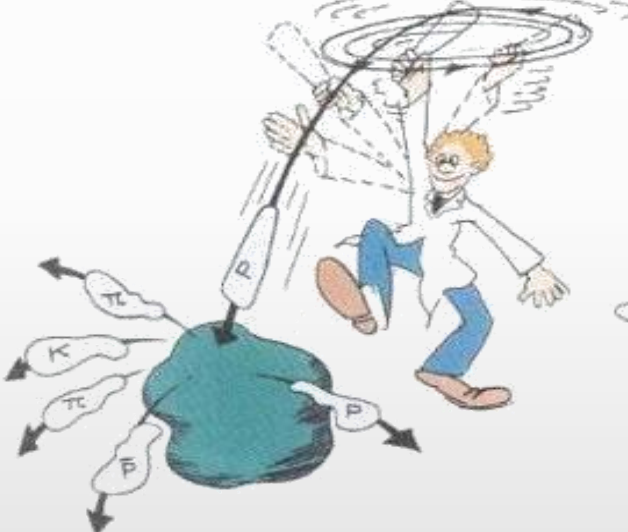
HADRON

QGP

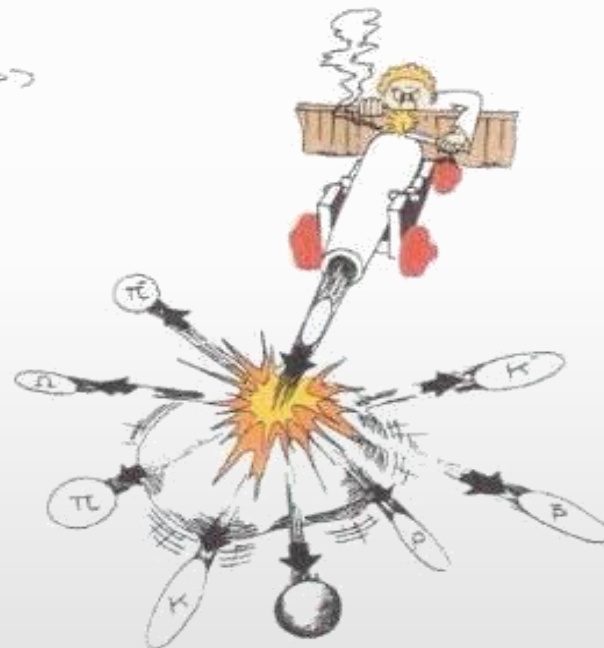


Increasing the beam energy over the last decades...

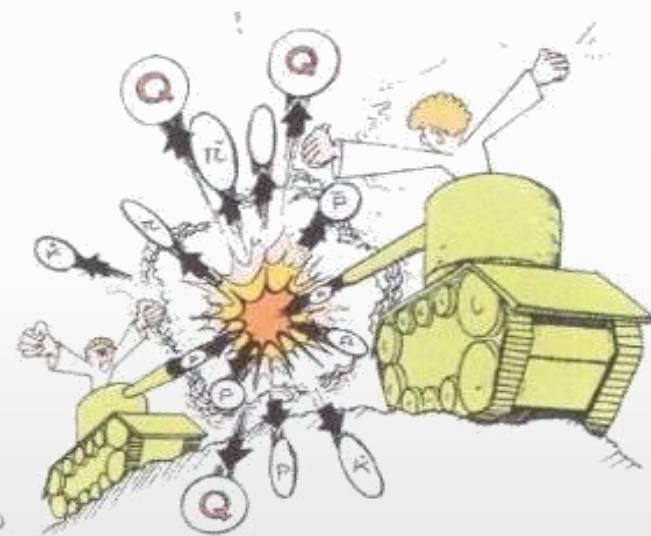
..from early fixed target experiments at GSI/Bevalac/JINR and SPS to collider experiments at RHIC and LHC.



Max mit seinem ersten großen
Teilchenbeschleuniger



J/ψ Charm



Max mit seinem größten
Teilchenbeschleuniger

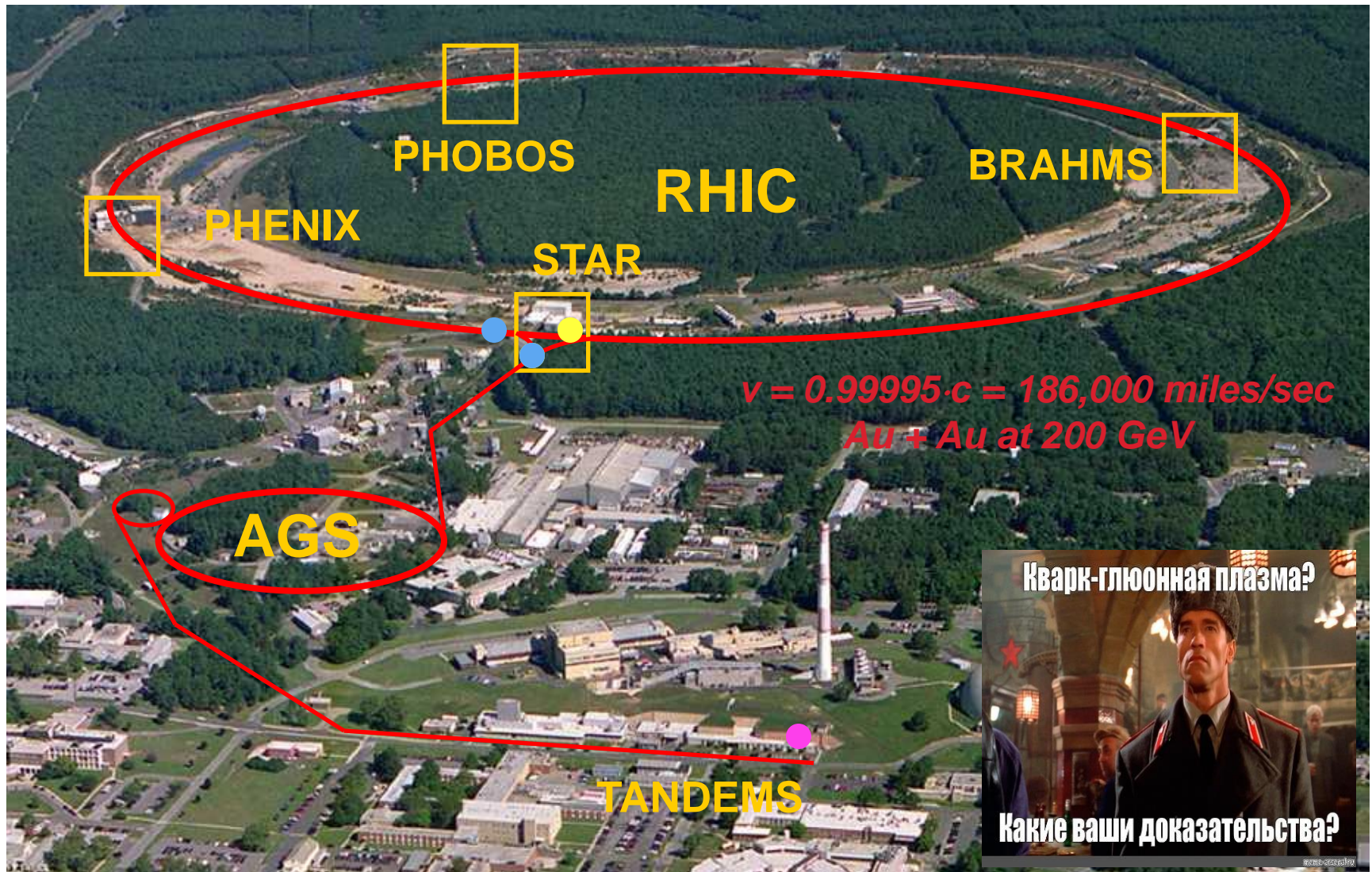
SIS, GSI Darmstadt, $\sqrt{s_{NN}} \sim 2.4 \text{ GeV}$

SPS, CERN, $\sqrt{s_{NN}} \sim 6-20 \text{ GeV}$

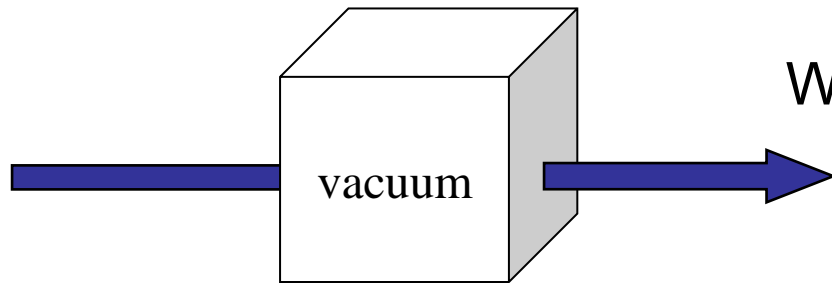
Brookhaven → RHIC $\sqrt{s_{NN}} \sim 3-200 \text{ GeV}$
(BES)
CERN → LHC $\sqrt{s_{NN}} = 5.02 \text{ TeV}$

2005: Quark-Gluon Plasma is a “perfect liquid”

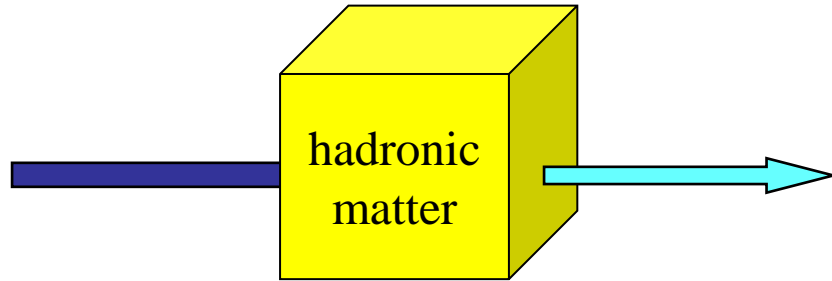
Relativistic Heavy-Ion Collider (BNL), Upton, NY (USA)



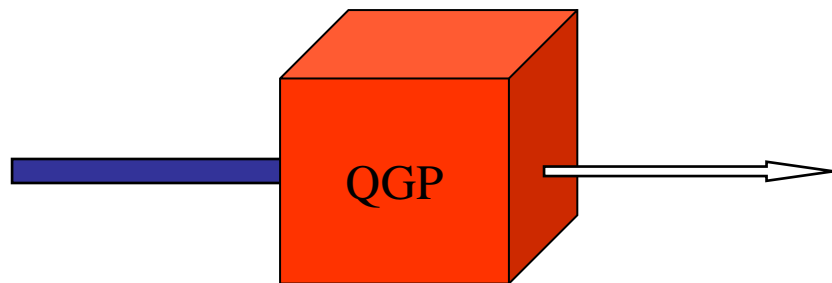
The good QCD matter probes should be:



Well understood in “p+p collisions”



Affected by hadronic matter,
in a well understood way,
which can be accounted for



Strongly affected by the dense
and
deconfined QCD medium...

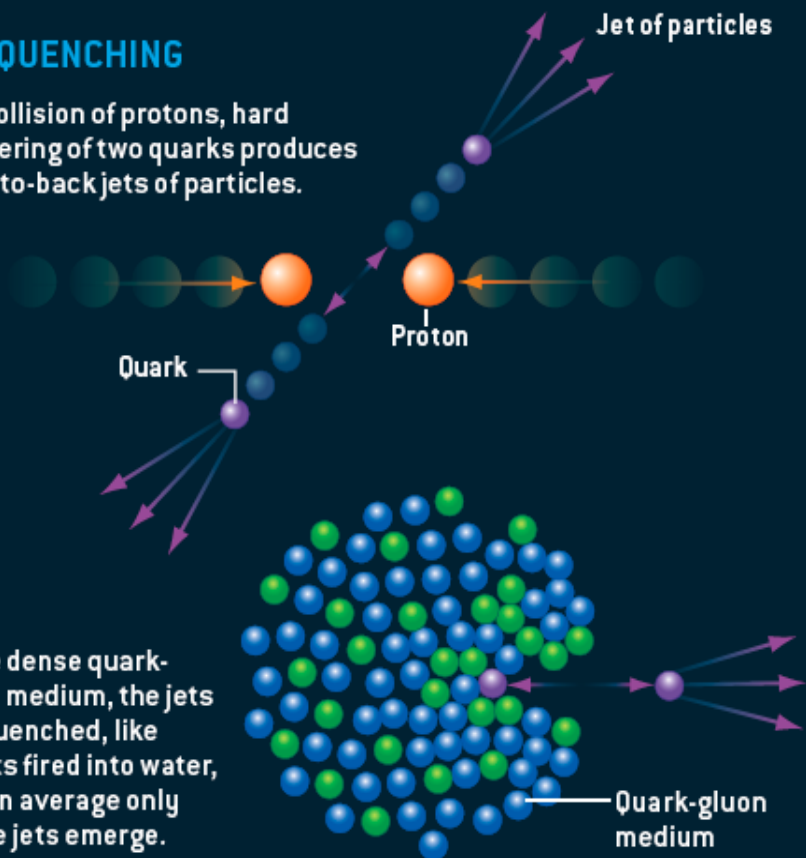
The sQGP Discovered at RHIC: 2005

EVIDENCE FOR A DENSE LIQUID

Two phenomena in particular point to the quark-gluon medium being a dense liquid state of matter: jet quenching and elliptic flow. Jet quenching implies the quarks and gluons are closely packed, and elliptic flow would not occur if the medium were a gas.

JET QUENCHING

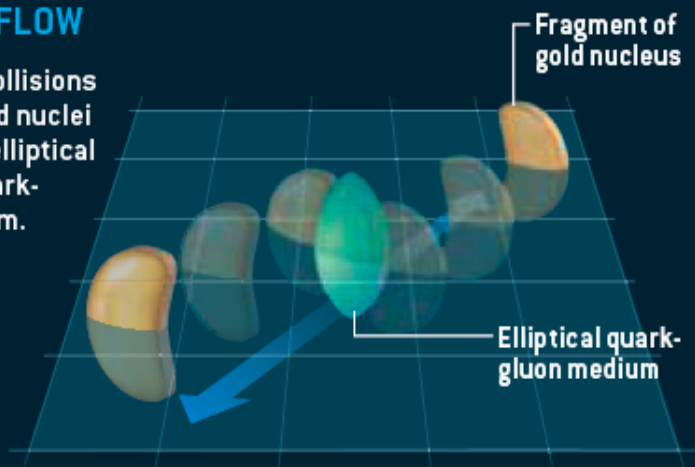
In a collision of protons, hard scattering of two quarks produces back-to-back jets of particles.



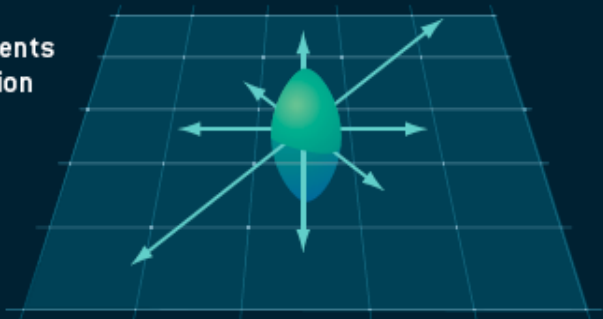
In the dense quark-gluon medium, the jets are quenched, like bullets fired into water, and on average only single jets emerge.

ELLIPTIC FLOW

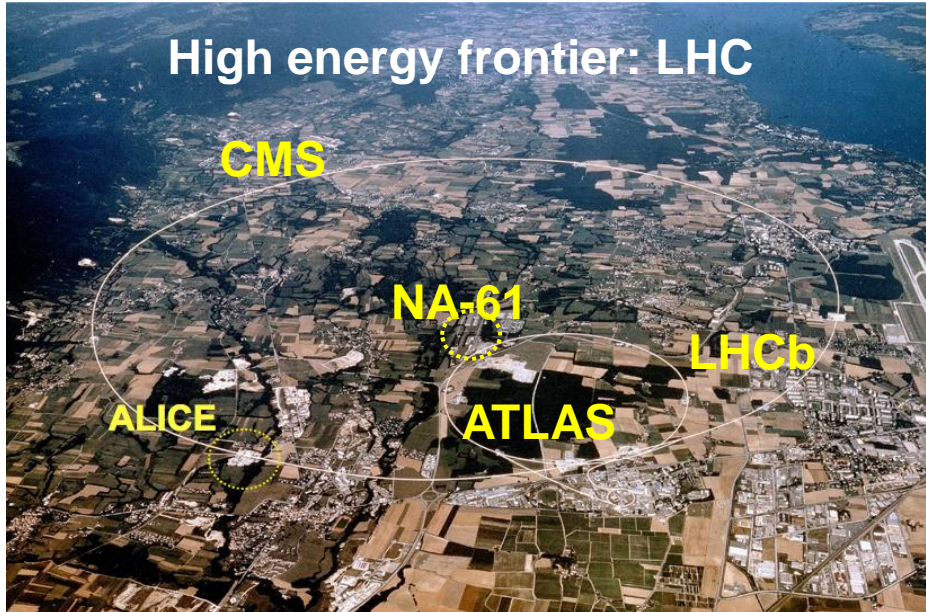
Off-center collisions between gold nuclei produce an elliptical region of quark-gluon medium.



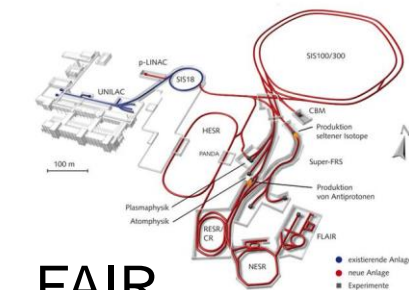
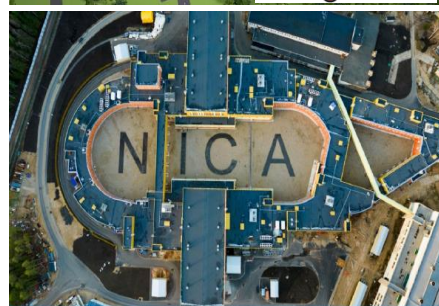
The pressure gradients in the elliptical region cause it to explode outward, mostly in the plane of the collision (arrows).



Relativistic Heavy-Ion Experiments



Low energy frontier: RHIC (BES), SPS
→ future facilities: FAIR (GSI), NICA



FAIR

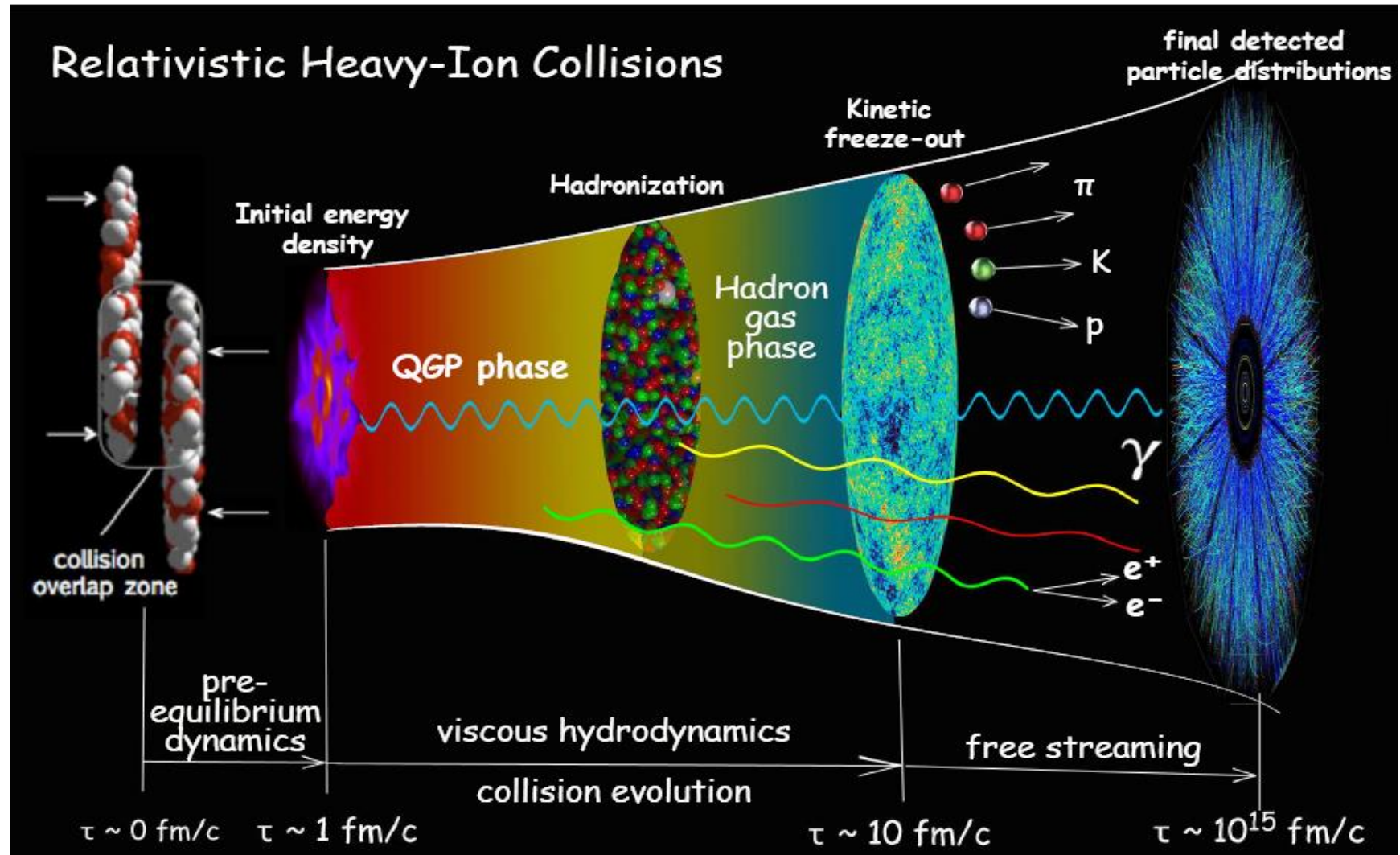


RHIC

→ By now all major LHC experiments have a heavy-ion program: LHCb took Pb-Pb data for the first time in November 2015.

Evolution of the system created in RHIC

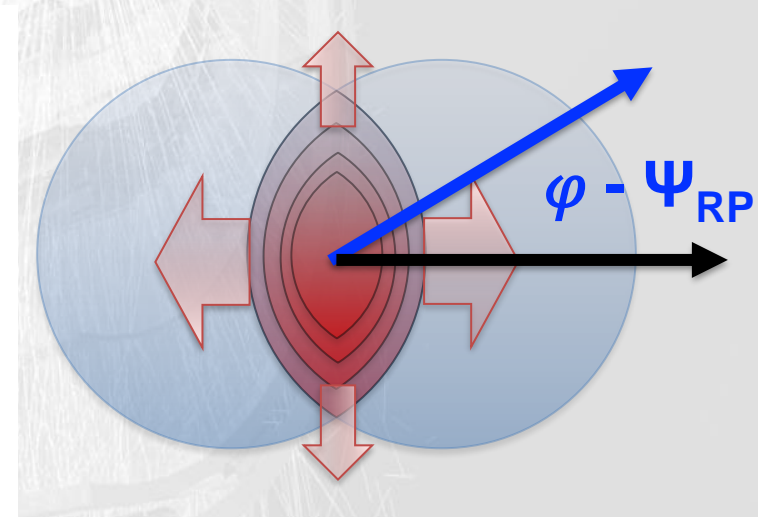
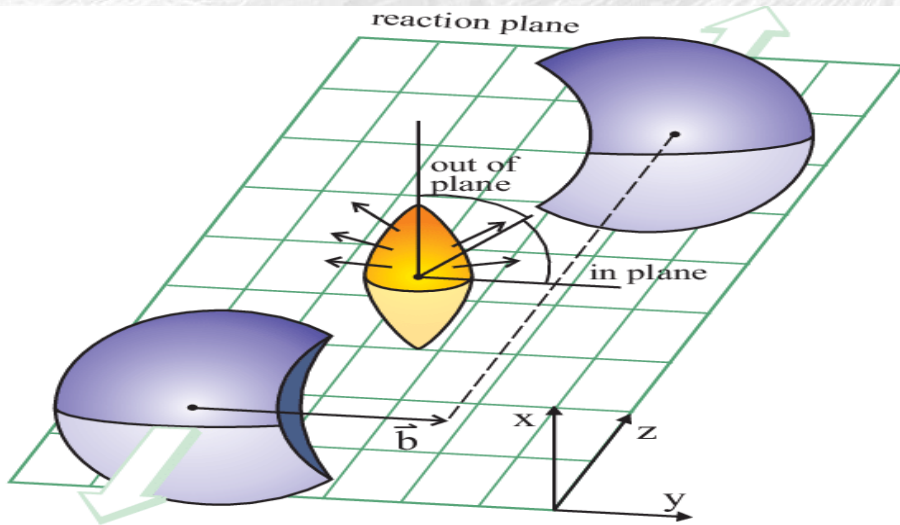
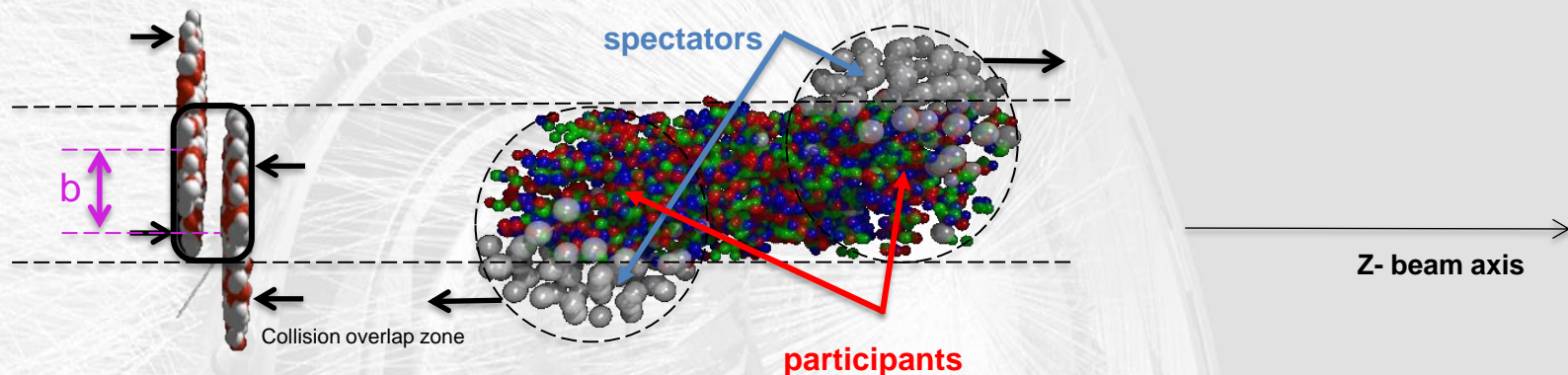
Fireball is $\sim 10^{-15}$ meters across and lives for 5×10^{-23} seconds



~ 400 nucleons in 10^{-22} seconds = 1000-30000 hadrons

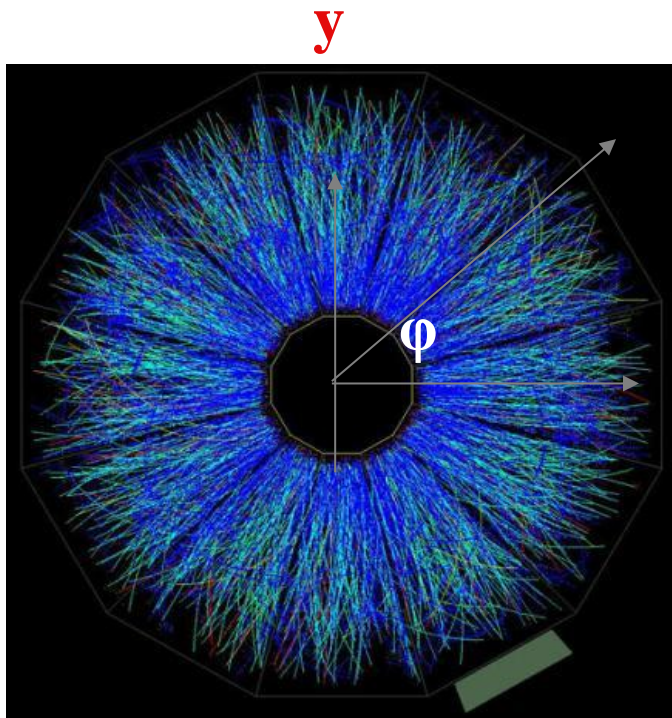
Characterising a heavy-ion collision

We can control a posteriori the geometry of the collision by selecting in **centrality**.
Centrality = fraction of the total hadronic cross section of a nucleus-nucleus collision, typically expressed in percentile, and related to the **impact parameter (b)**

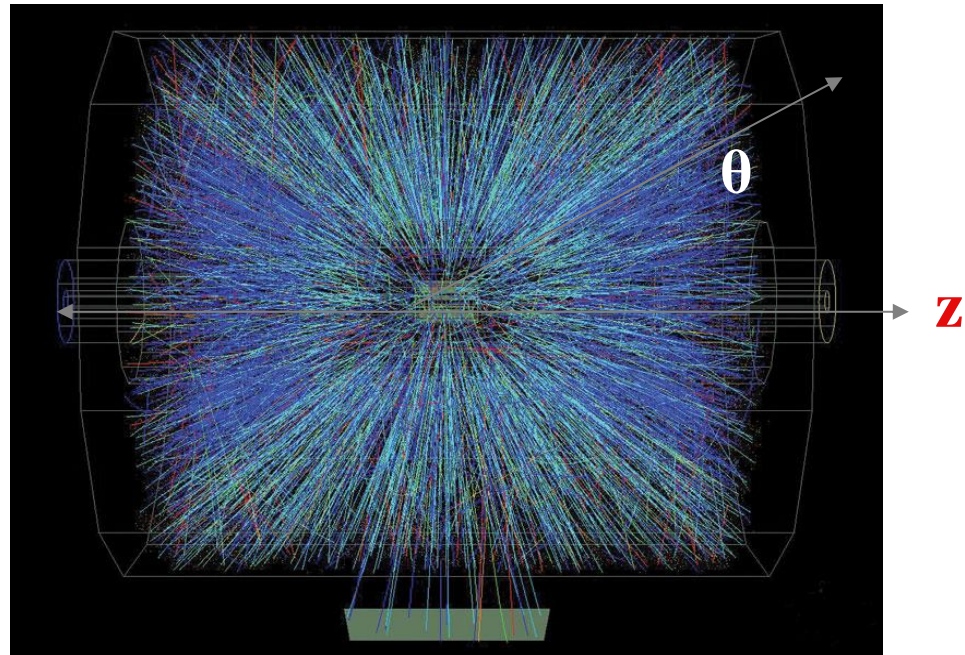


Definition of kinematical variables

Momentum , azimuthal angle ϕ and pseudo-rapidity (η) of the emitted particles



x



z

$$\eta = \frac{1}{2} \log \left(\frac{|\vec{p}| + p_z}{|\vec{p}| - p_z} \right) = -\log \left[\tan \left(\frac{\theta}{2} \right) \right]$$

$$p_T = \sqrt{p_x^2 + p_y^2}$$

p_T is generated in the collision (while p_z is already present “before the collision”)

MPD experiment at NICA

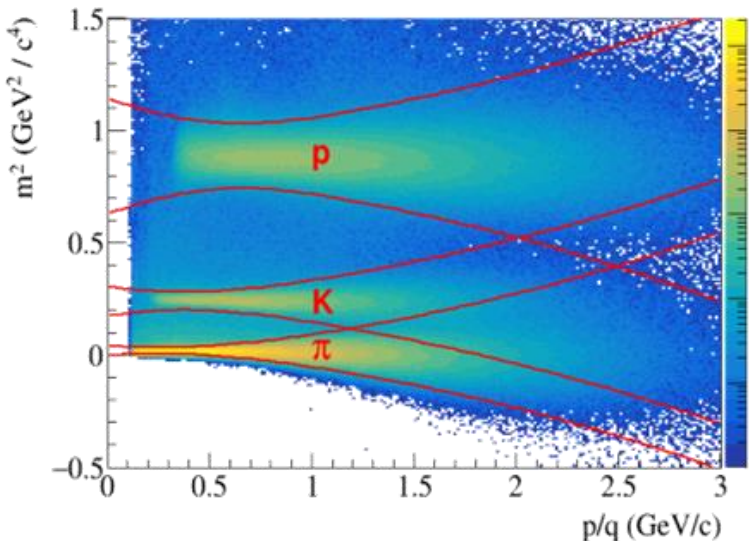
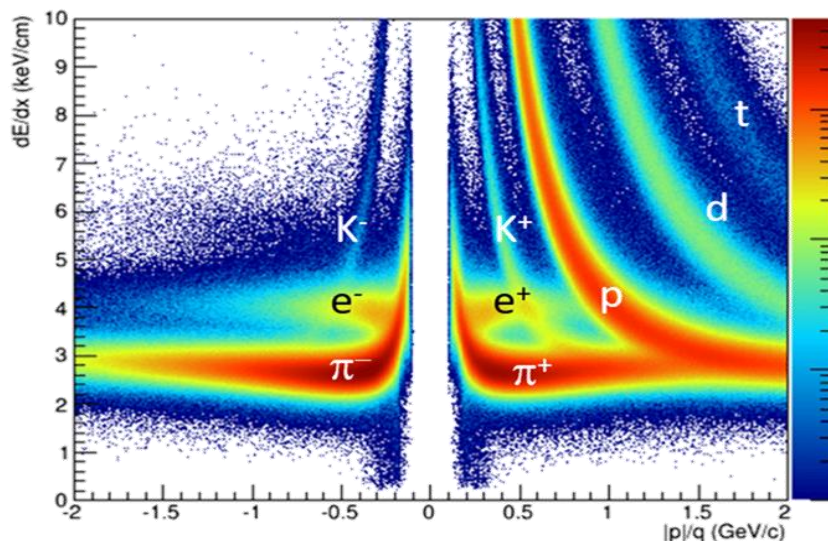
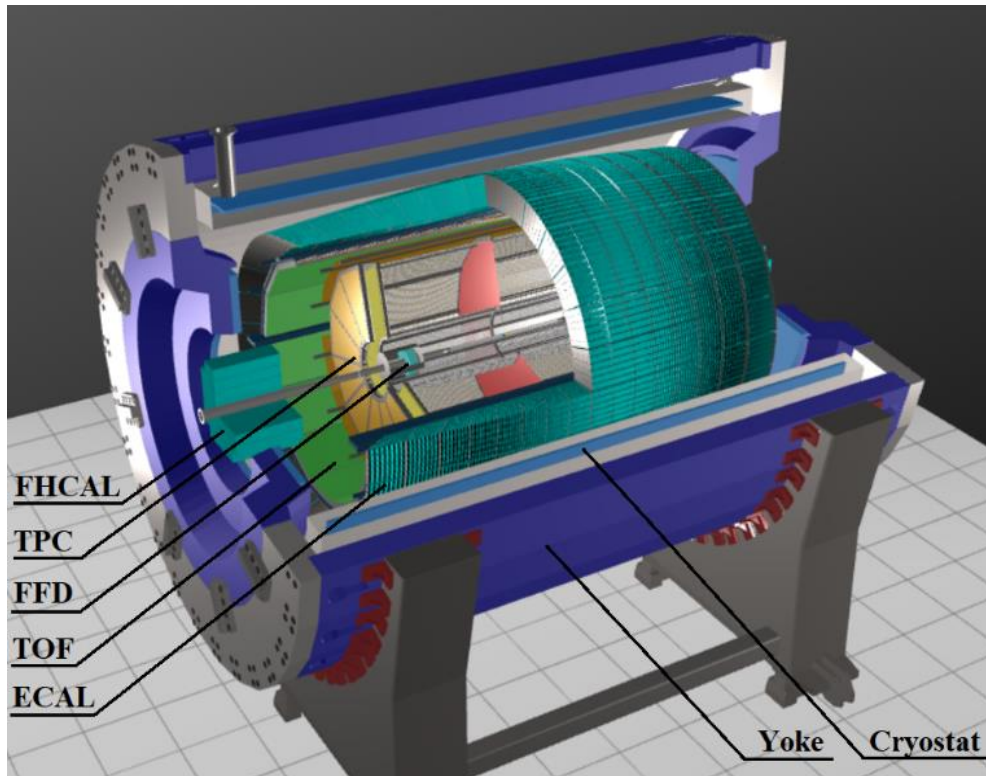
Main subsystems at Stage-I:

TPC ($|\eta| \leq 1.6$): charged particle tracking + momentum reconstruction + dE/dx identification

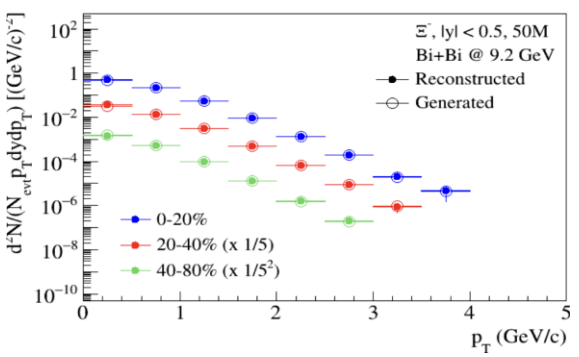
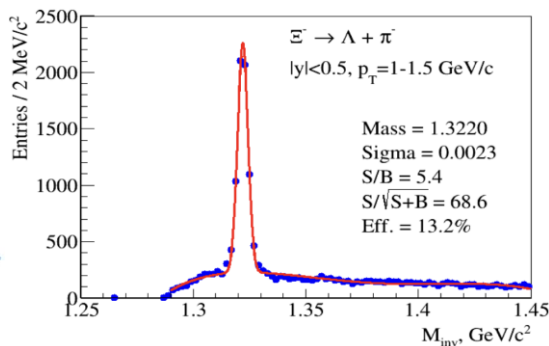
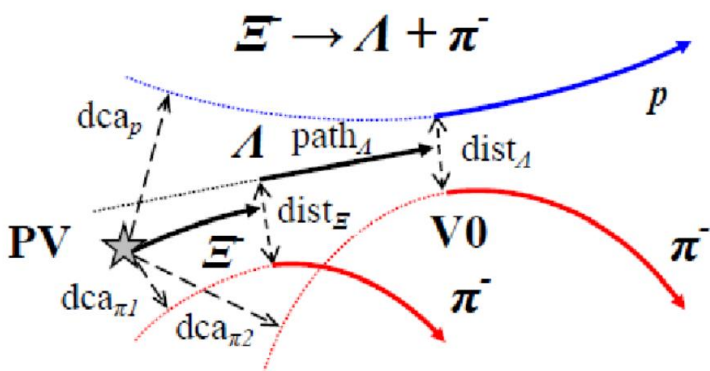
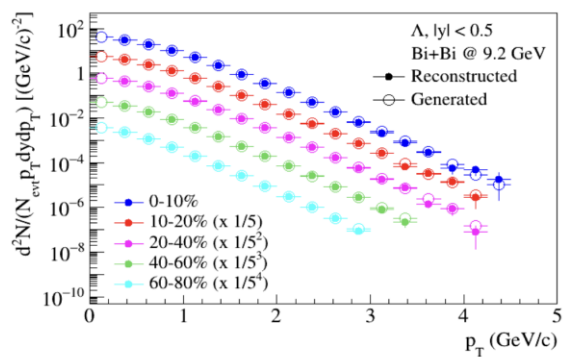
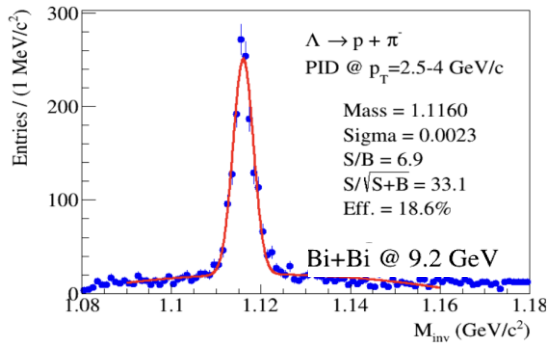
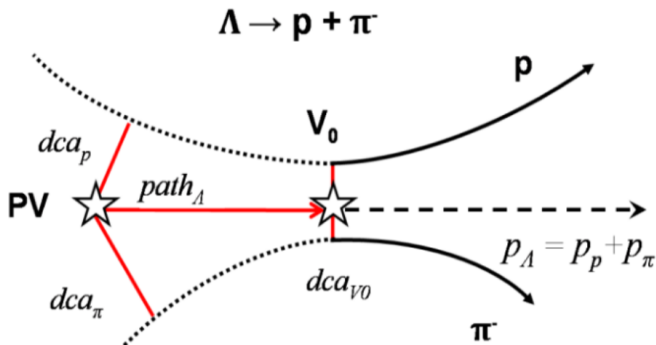
TOF ($|\eta| \leq 1.4$): charged particle identification

ECal ($2.9 < |\eta| < 1.4$): energy and PID for γ/e^\pm

FHCAL ($2 < |\eta| < 5$) and **FFD** ($2.9 < |\eta| < 3.3$): event triggering + event geometry



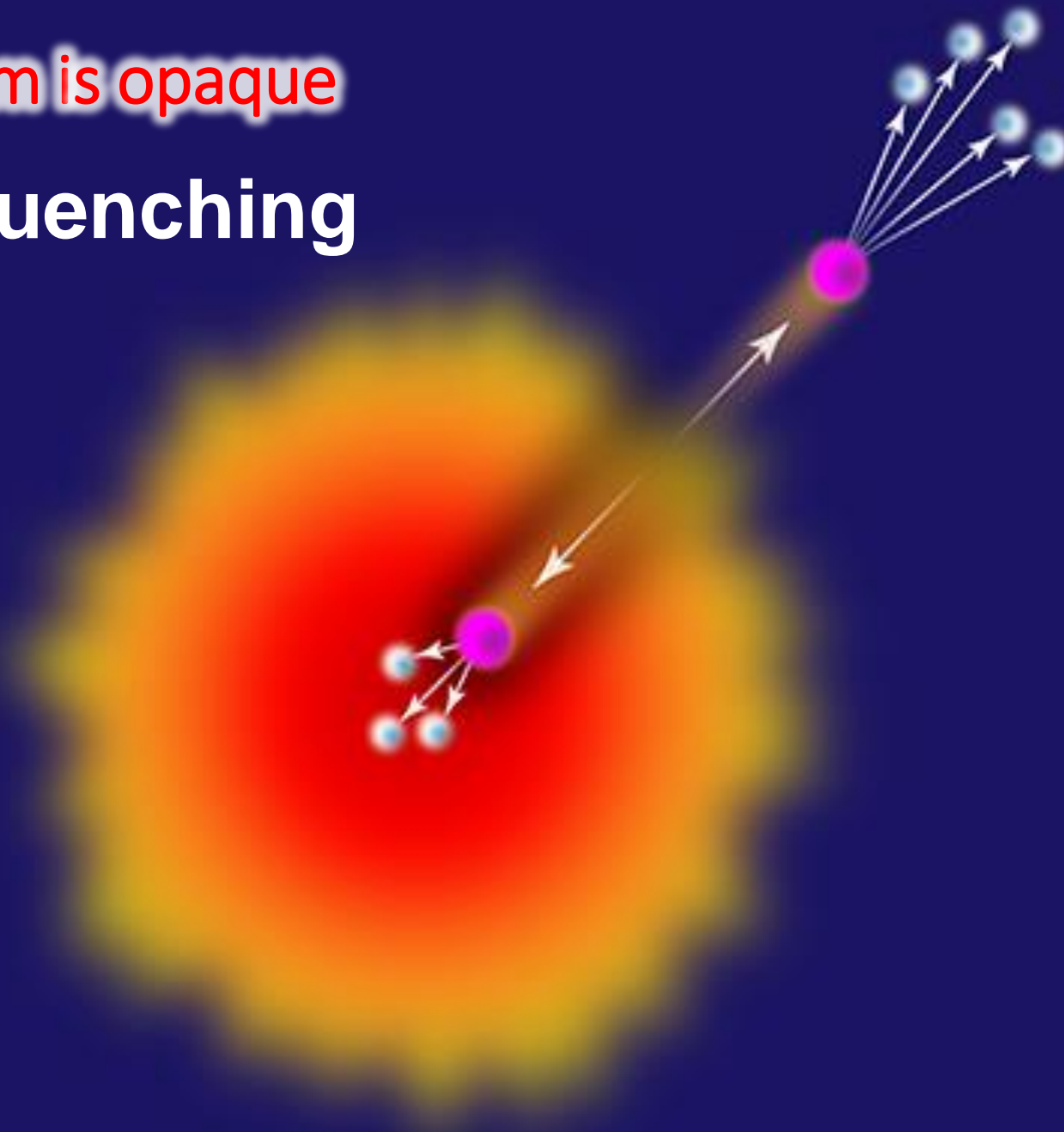
PID via Topology and Invariant Mass



$$\begin{aligned} M^2 &= (E_1 + E_2)^2 - \|\mathbf{p}_1 + \mathbf{p}_2\|^2 \\ &= m_1^2 + m_2^2 + 2(E_1 E_2 - \mathbf{p}_1 \cdot \mathbf{p}_2). \end{aligned}$$

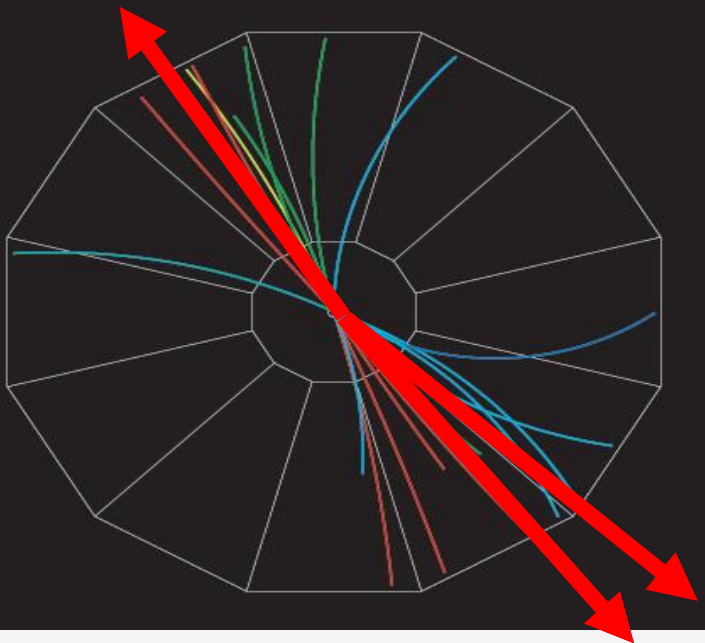
medium is opaque

Jet quenching

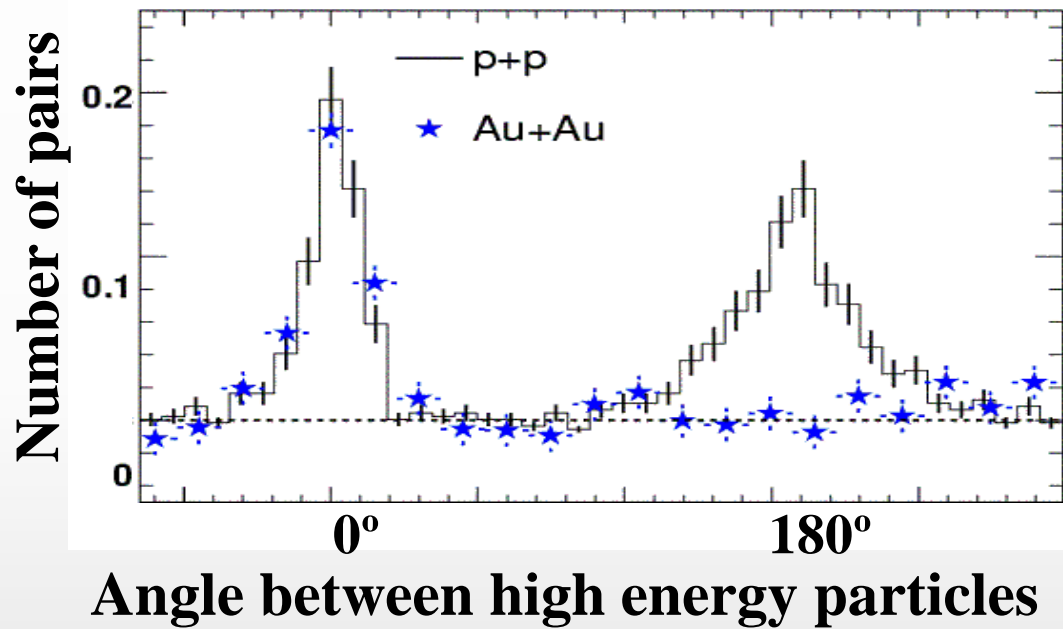


RHIC Experiment: “Jet quenching”

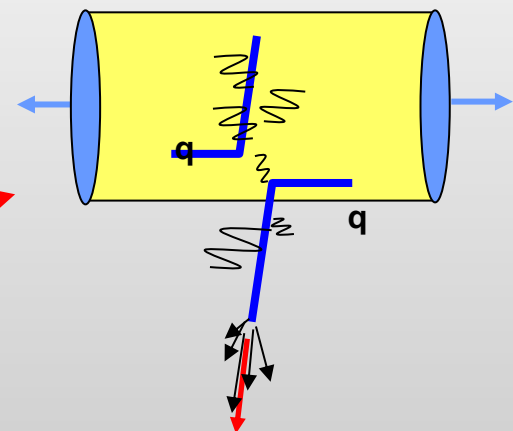
proton-proton jet event



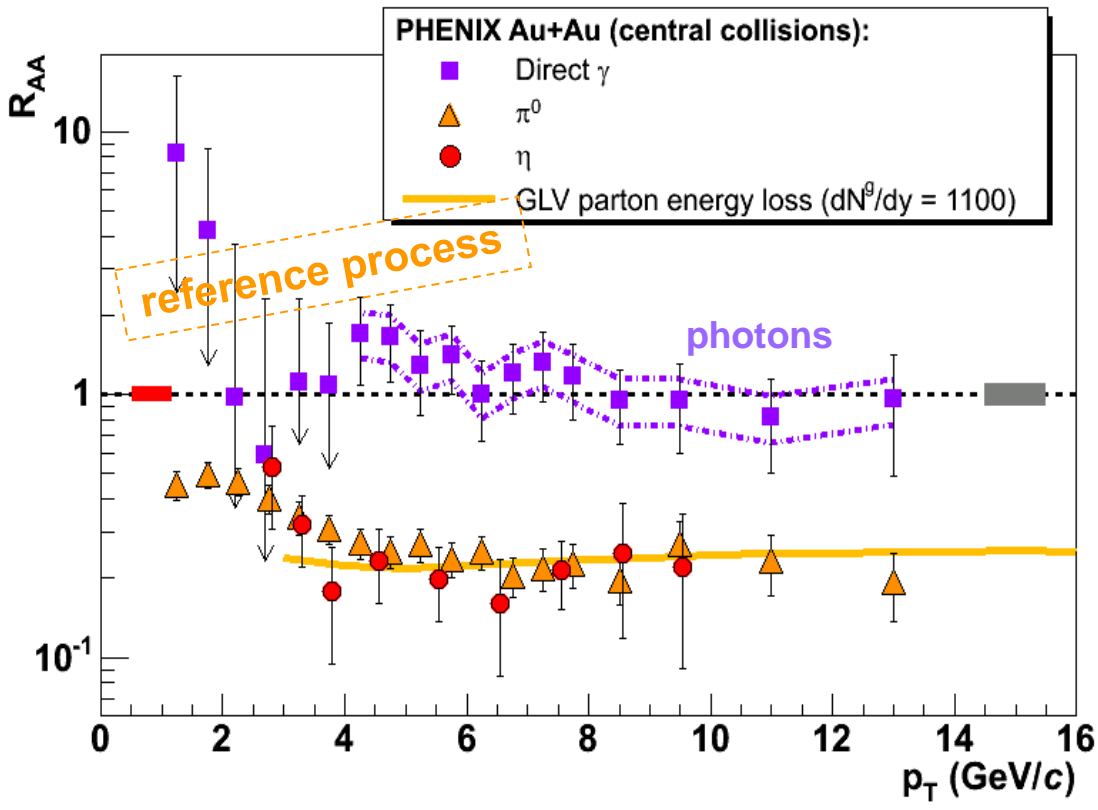
Analyze by measuring (azimuthal) angle between pairs of particles



- In Au-Au collisions we see only one “jet” at a time !
- How can this happen ?
- Jet quenching!



The nuclear modification factor: R_{AA}



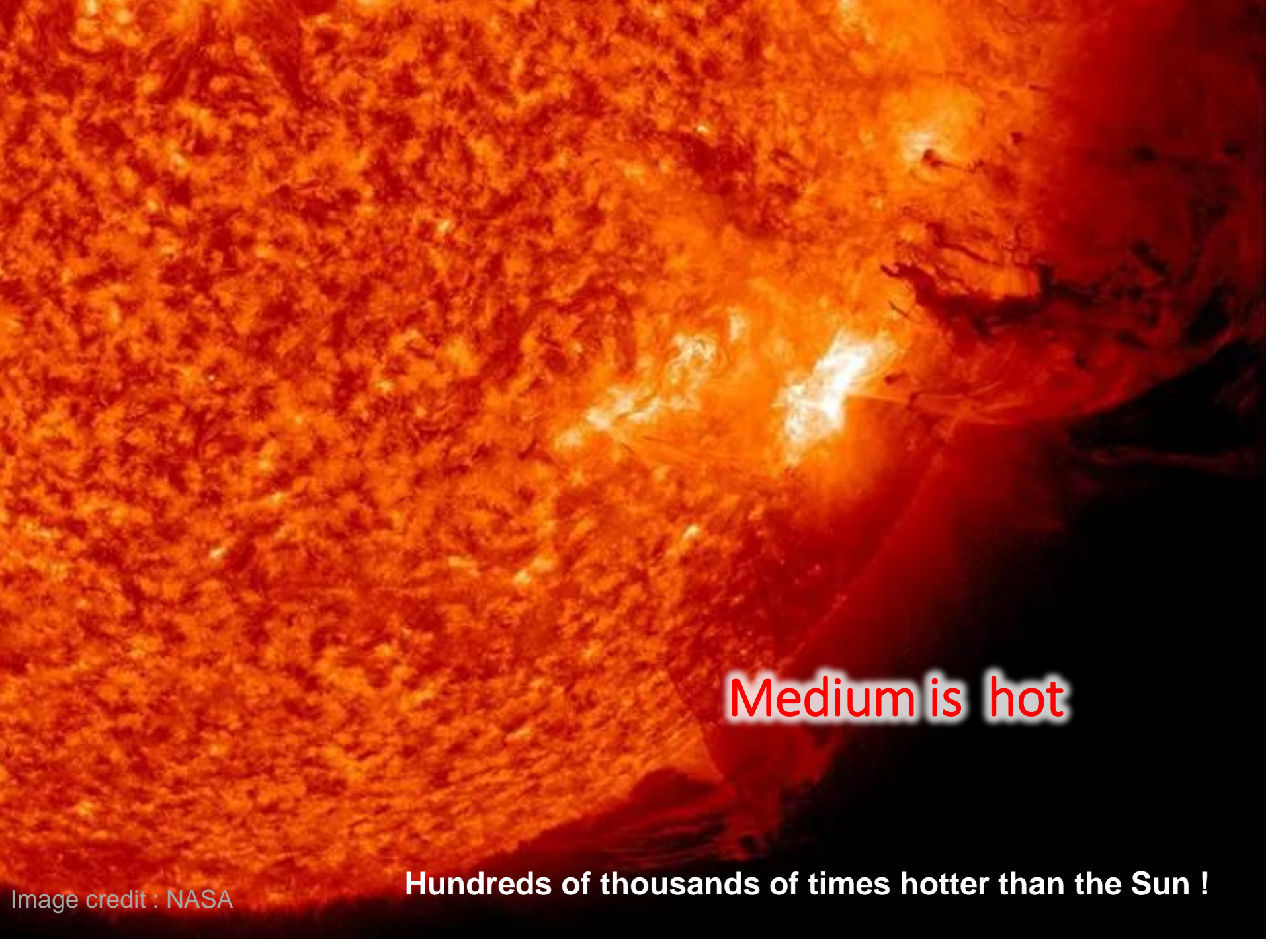
If $R_{AA} < 1$ at high p_T
 → the medium is opaque to the passage of partons
 → parton-medium final state interactions, energy loss, modification of fragmentation in the medium

$R_{AA} = 1$ at high p_T
 → the medium is transparent to the passage of partons

$$R_{AA} = \frac{d\langle N_{AA} \rangle / dp_T}{N_{coll} \cdot dN_{pp} / dp_T}$$

The **meson yield** in central Au-Au is 5 times lower than expected from pp collisions

the **direct photons** are not affected by the dense medium

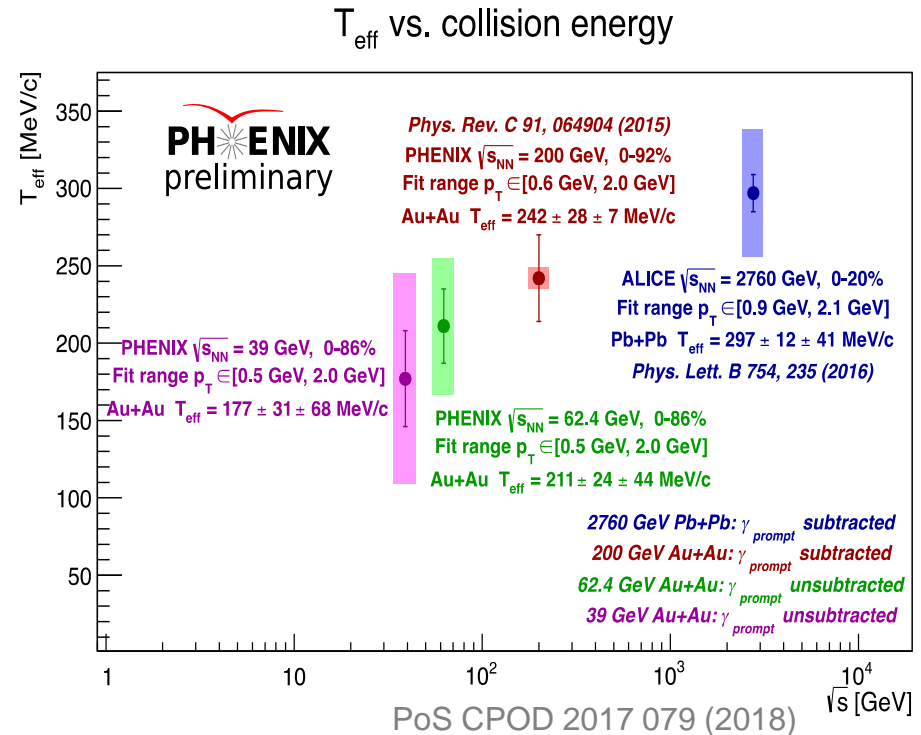
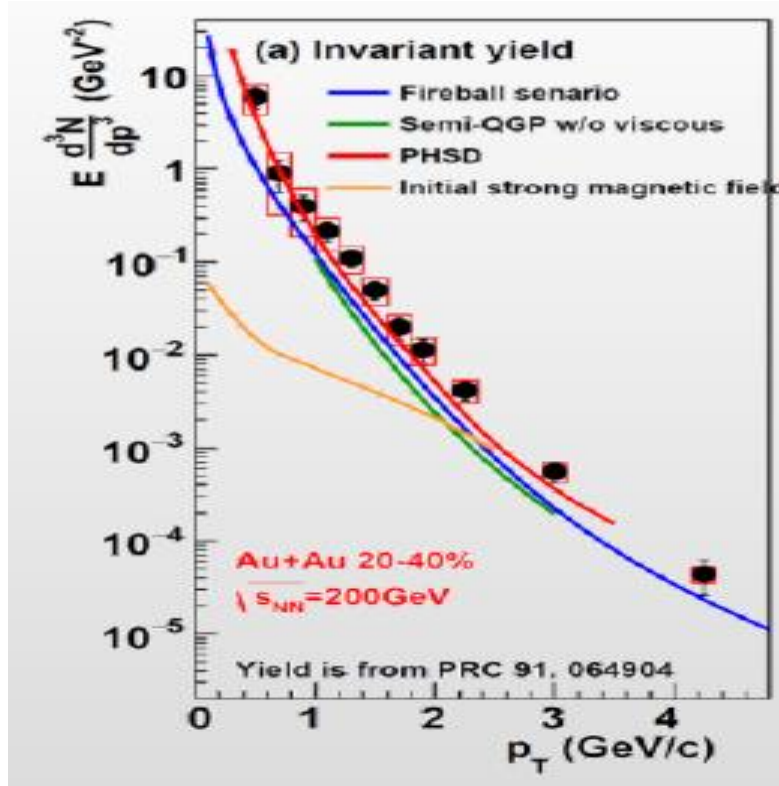
A high-resolution image of the Sun's surface, showing a complex pattern of bright, turbulent plasma filaments against a dark background. Two distinct solar flares are visible: one on the left side and another larger, more intense one on the right side, both emitting bright white and yellow light.

Medium is hot

Hundreds of thousands of times hotter than the Sun !

Image credit : NASA

Thermal photons in A+A collisions



- Measure the spectrum of thermal photons (non-interacting) emitted from the source.
- The spectrum will display the average temperature over the full lifetime of the partonic source.
- Determining the initial temperature requires modeling.

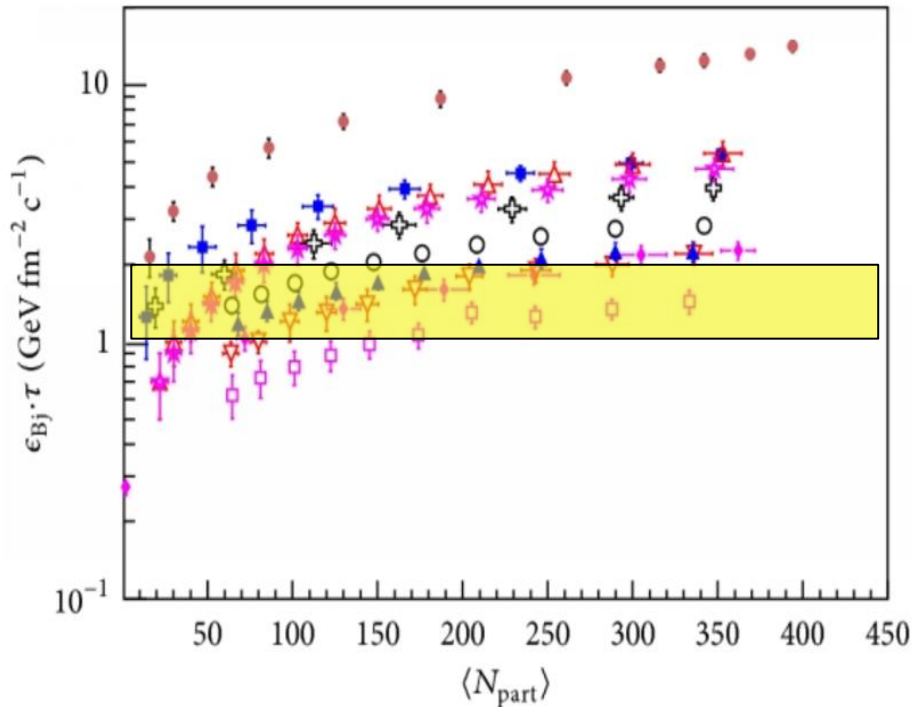
p_T slope \Rightarrow Temperature

Medium is dense

Pack the entire Earth inside a stadium !



Energy Density



PHENIX Au+Au BES

- △ 200 GeV
- ★ 130 GeV
- 39 GeV
- ▲ 27 GeV
- ▽ 19 GeV
- 7.7 GeV

- CMS (Pb+Pb, $\sqrt{s_{\text{NN}}} = 2.76$ TeV)
- STAR (Au+Au, $\sqrt{s_{\text{NN}}} = 200$ GeV)
- ✚ STAR (Au+Au, $\sqrt{s_{\text{NN}}} = 62.4$ GeV)
- ◆ NA49 (Pb+Pb, $\sqrt{s_{\text{NN}}} = 17.2$ GeV)

$$\varepsilon_0 = \frac{dE_T}{dy} \frac{1}{\tau_0 \pi R^2}$$

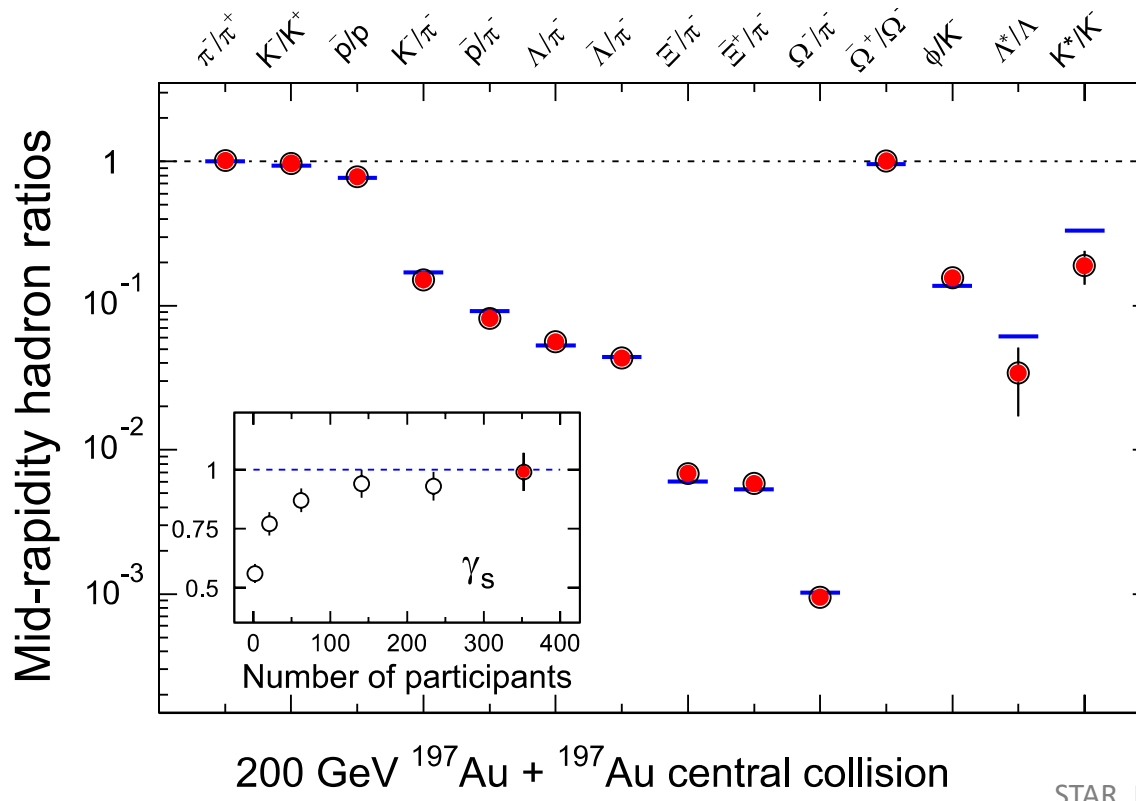
$$\tau_0 \sim 1 \text{ fm}/c, R \approx 1.2 A^{1/3} \text{ fm}$$

$$\varepsilon_0 = 4.9 \pm 0.3 \text{ GeV/fm}^3$$

Critical condition for QGP satisfied.

Chemical and Thermal Equilibrium?

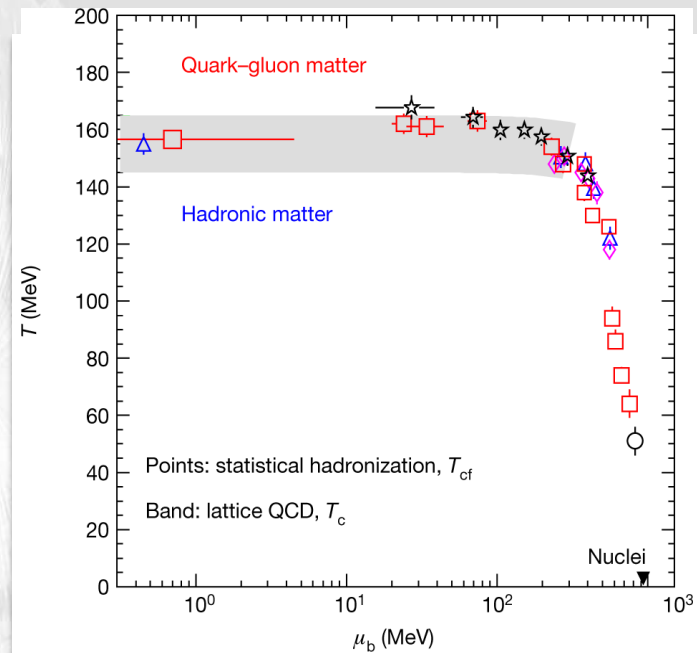
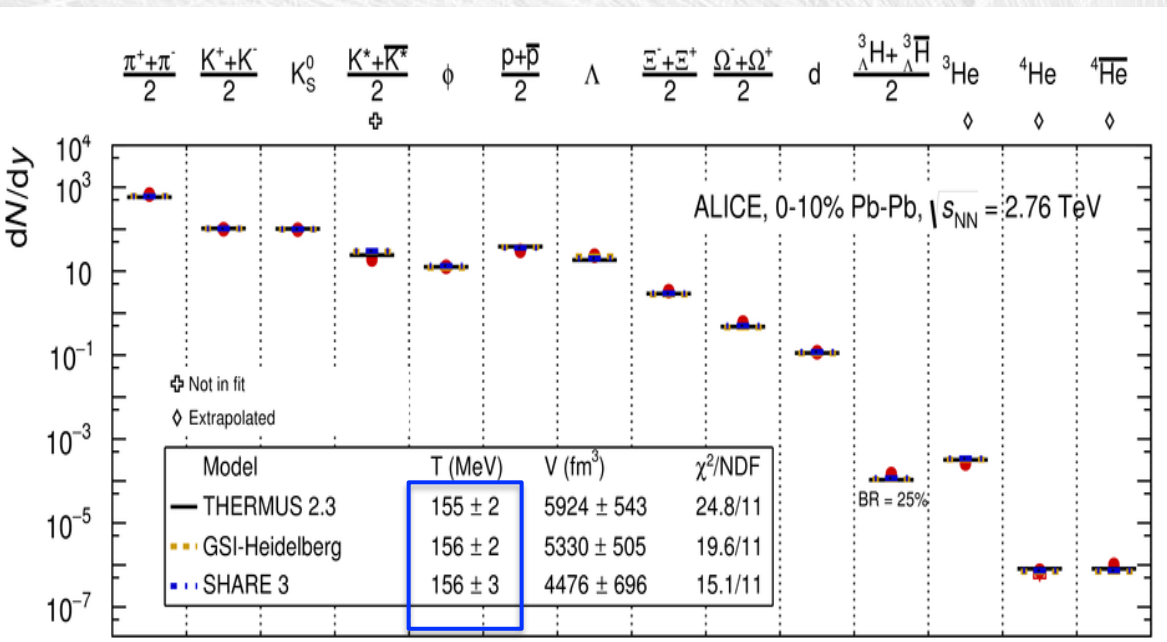
Particle yields freeze



Particle ratios described very well by statistical model assuming thermal and chemical equilibrium

Chemical freeze-out temperature - LHC

[Nature](#) volume 561, pages 321–330 (2018)



Production of (most) light-flavour hadrons (and anti-nuclei) is described ($\chi^2/\text{ndf} \sim 2$) by thermal models with a **single chemical freeze-out temperature, $T_{ch} \approx 156 \text{ MeV}$**

→ Approaches the critical temperature roof from lattice QCD: **limiting temperature** for hadrons!

→ the success of the model in fitting yields over 10 orders of magnitude supports the picture of a system in **local thermodynamical equilibrium**

It's perfect liquid

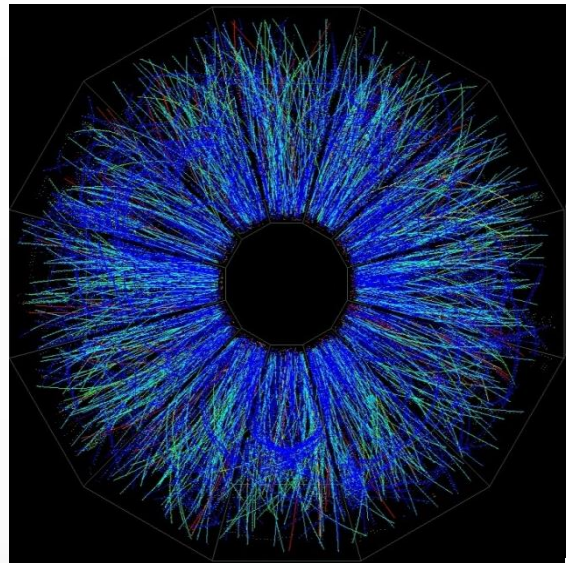
Lowest viscosity possible !



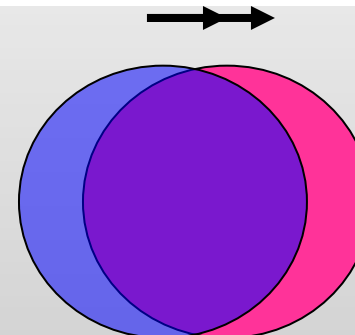
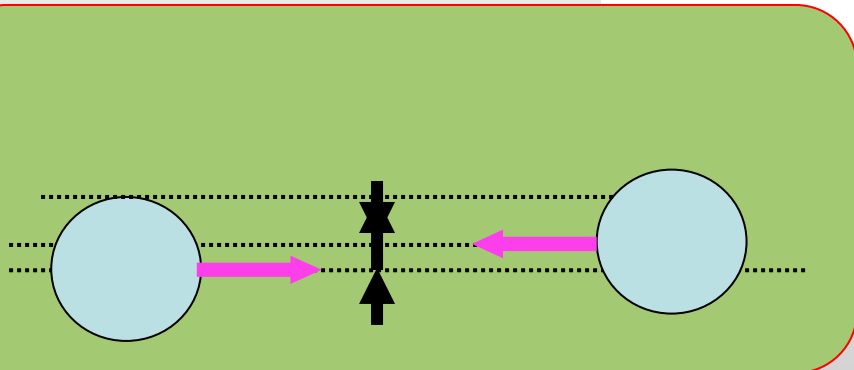
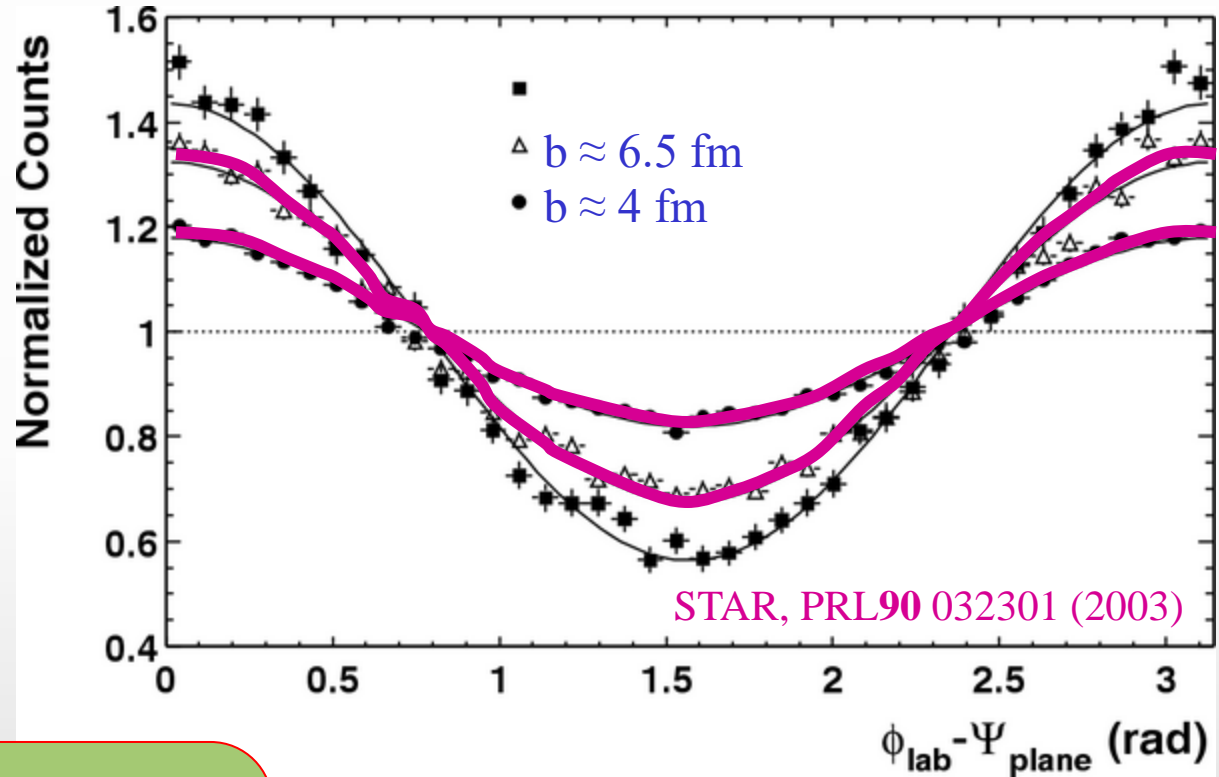
Image credit : SmileTemplates

Azimuthal distributions at RHIC

$$\frac{dN}{d\phi} \propto \left(1 + 2 \sum_{n=1} v_n \cos[n(\phi - \Psi_n)] \right)$$

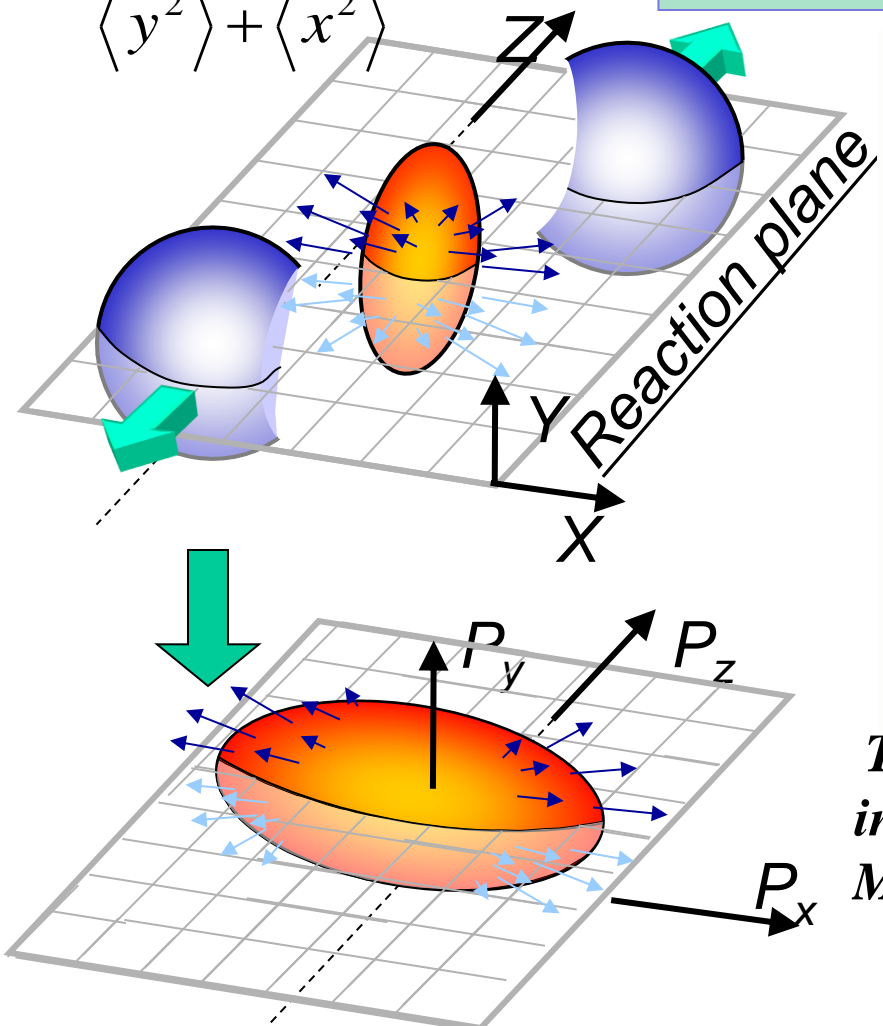


mid“central” collisions



$$\varepsilon = \frac{\langle y^2 \rangle - \langle x^2 \rangle}{\langle y^2 \rangle + \langle x^2 \rangle}$$

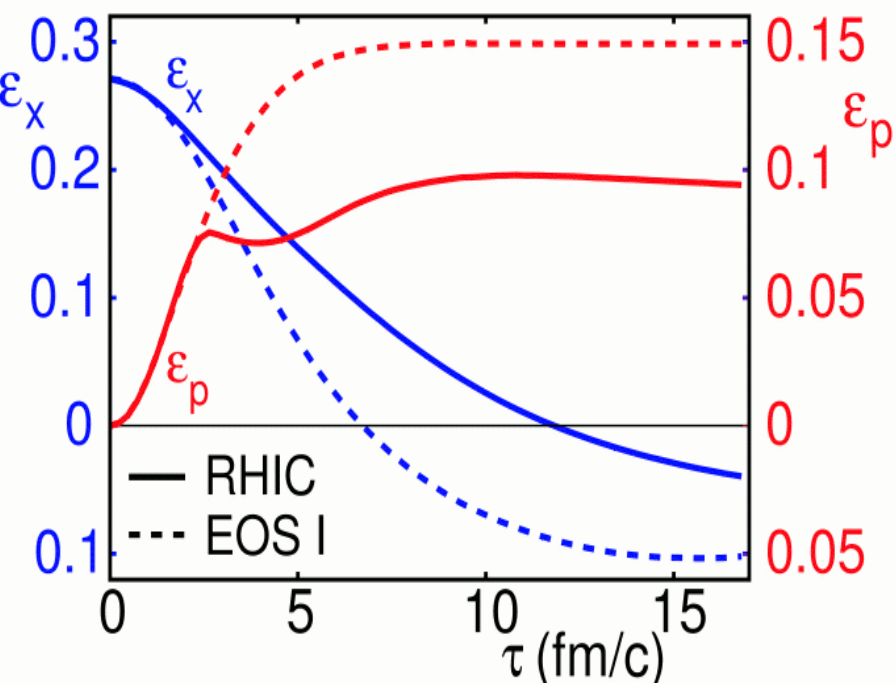
2005 - Elliptic Flow at RHIC



$$v_2 = \frac{\langle p_x^2 \rangle - \langle p_y^2 \rangle}{\langle p_x^2 \rangle + \langle p_y^2 \rangle}$$

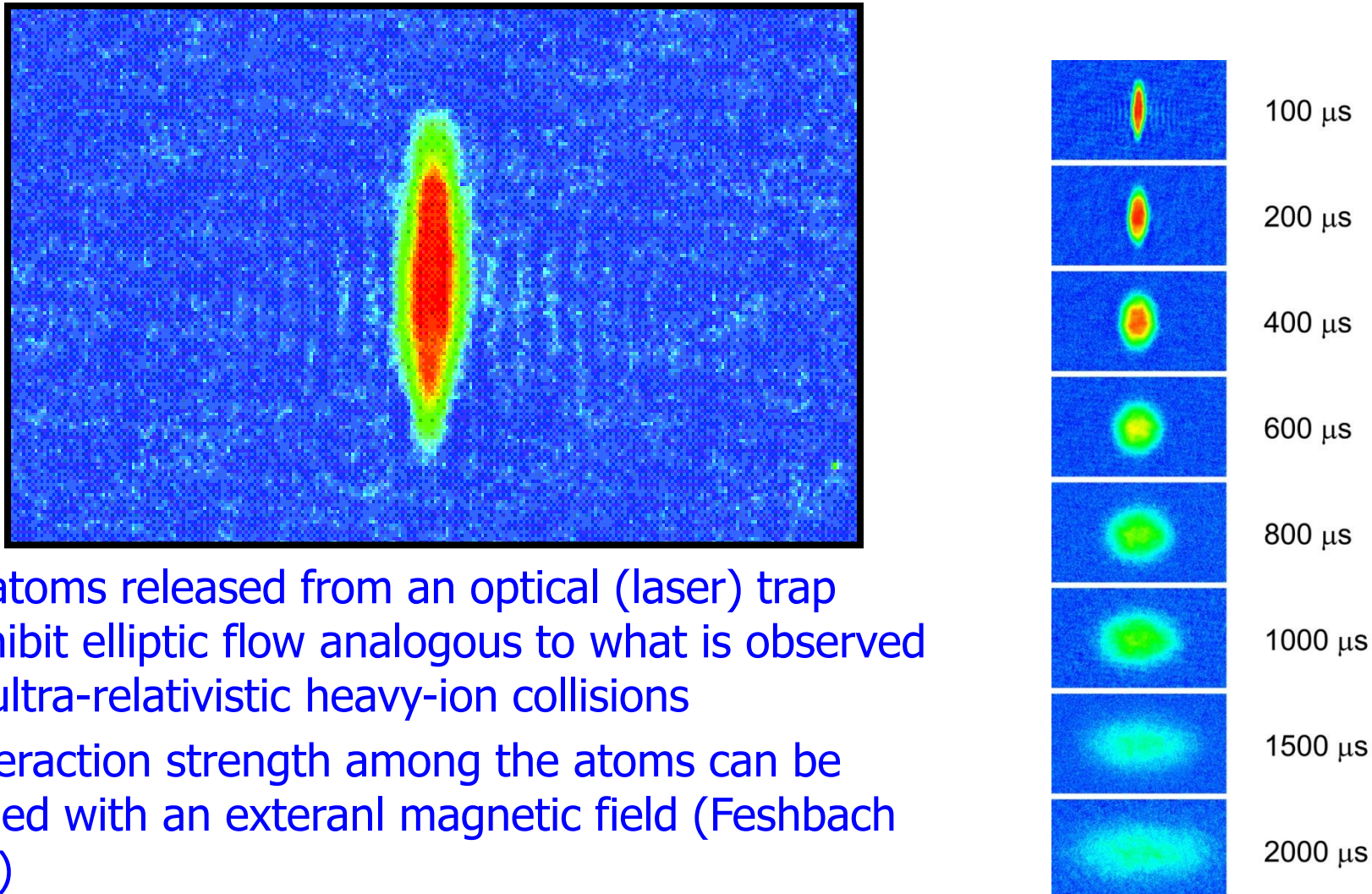


$$v_2 = \langle \cos(2[\varphi - \Psi_R]) \rangle$$



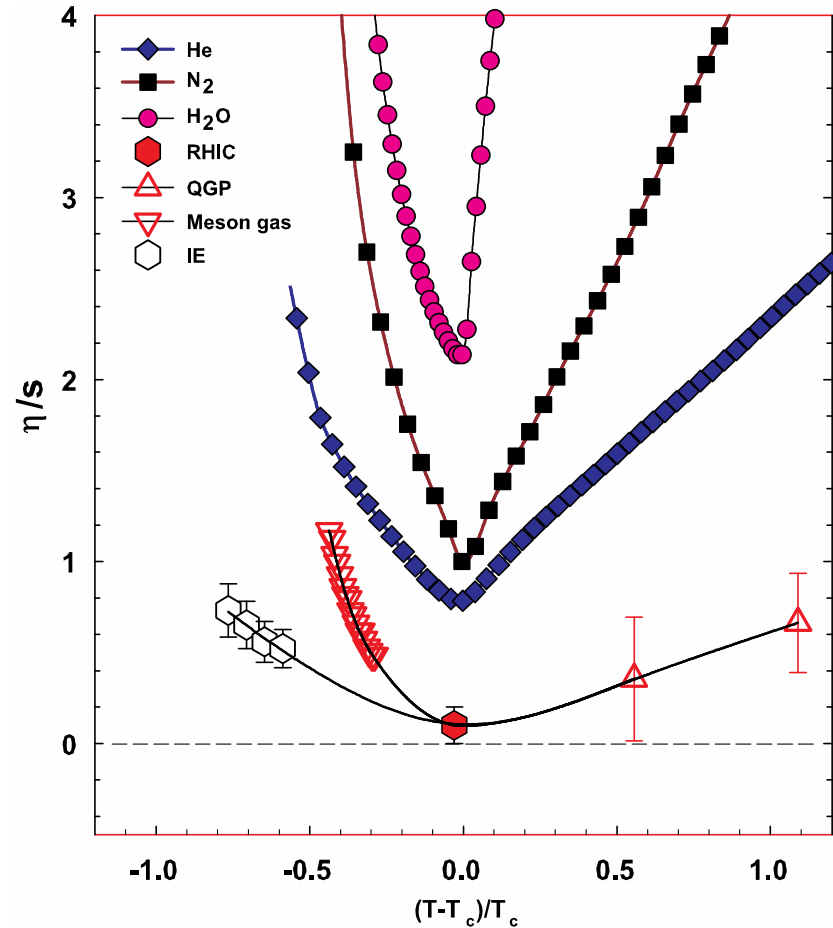
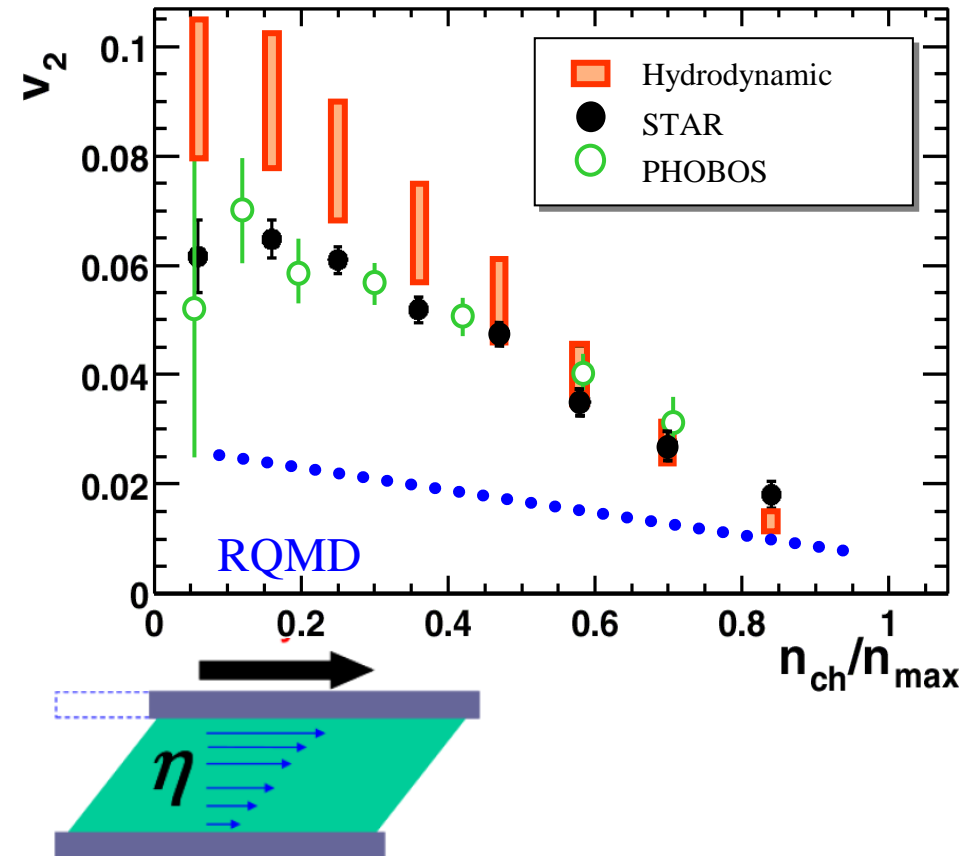
The initial spatial anisotropy evolves (via interactions and density gradients) → Momentum-space anisotropy

Elliptic Flow: ultra-cold Fermi-Gas



- Li-atoms released from an optical (laser) trap exhibit elliptic flow analogous to what is observed in ultra-relativistic heavy-ion collisions
- Interaction strength among the atoms can be tuned with an external magnetic field (Feshbach res)
- Elliptic flow is a general feature of strongly interacting systems?

Perfect Liquid at RHIC

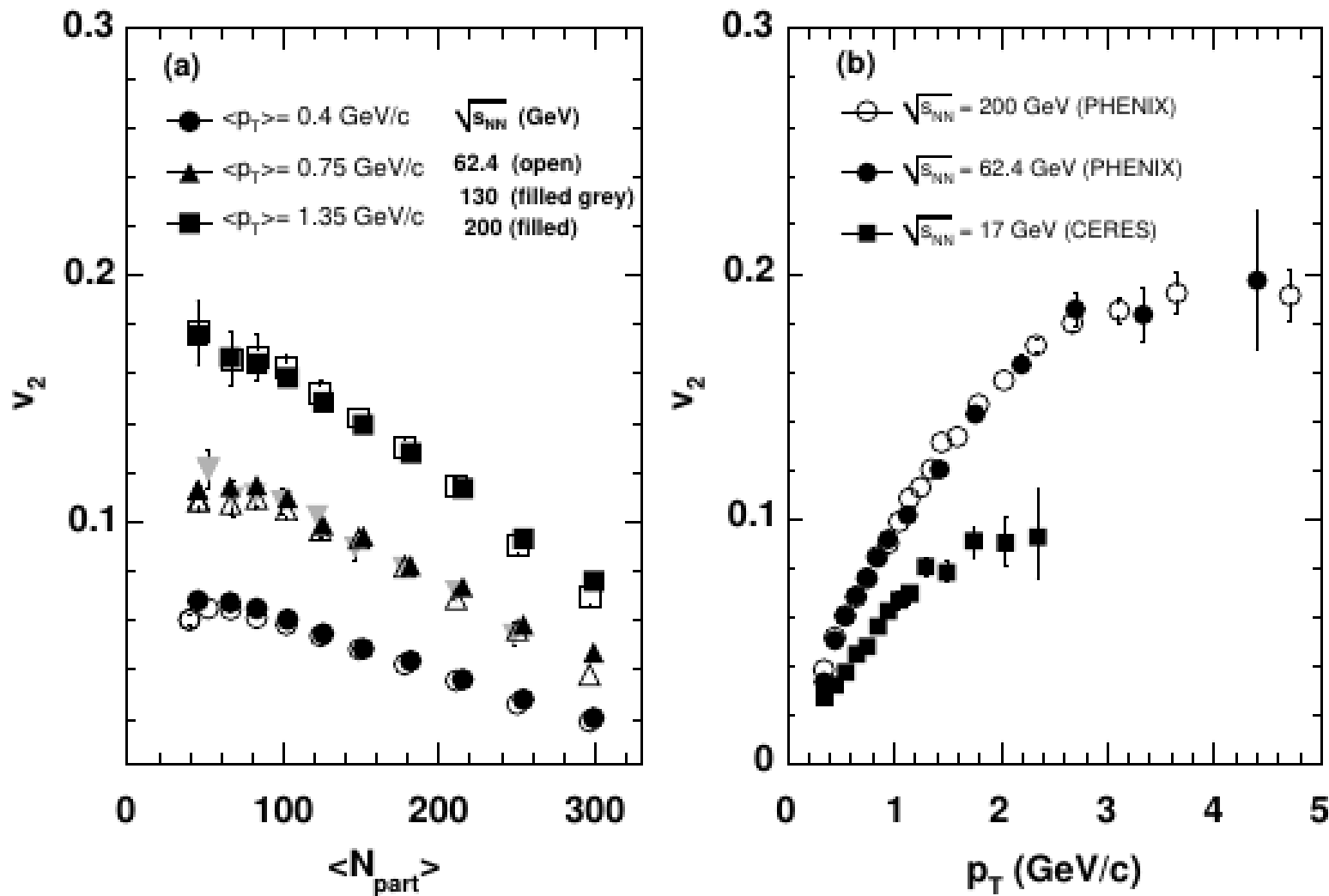


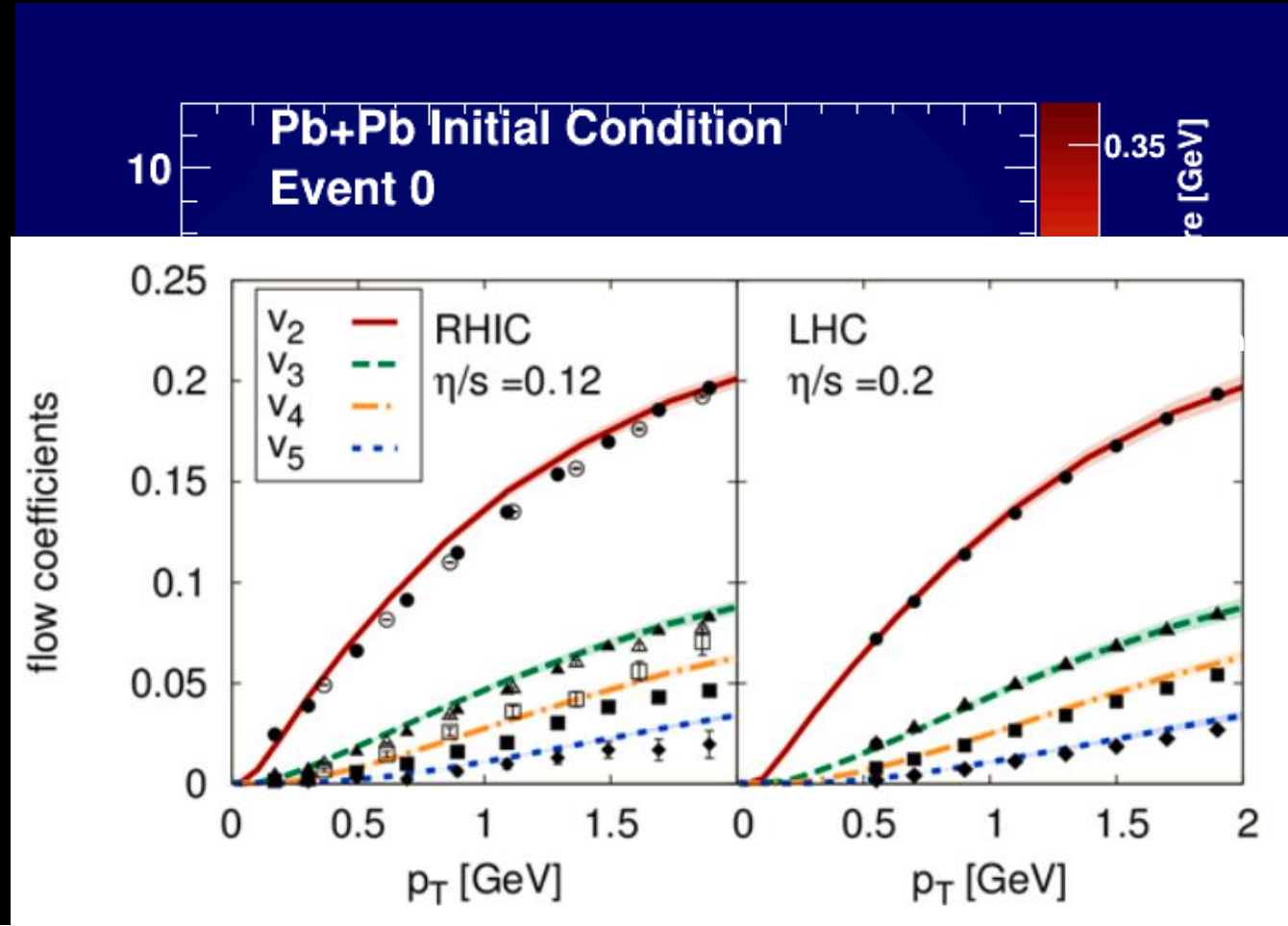
R. Lacey , A. Taranenko, PRL 98 092301 (2007)

Shear Viscosity – resistance to deformation, flow

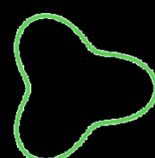
Data approaching Hydro for central collisions
viscosity extracted close to the lowest value set by quantum limit.

Elliptic Flow at RHIC/SPS

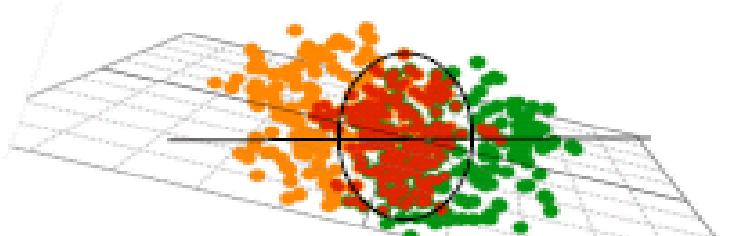




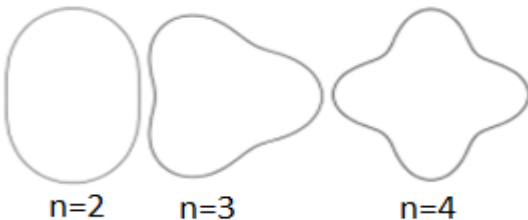
$$\frac{dN}{d\phi} = 1 + 2v_2 \cos[2(\phi - \Psi_2)] + 2v_3 \cos[3(\phi - \Psi_3)] + 2v_4 \cos[4(\phi - \Psi_4)] + 2v_5 \cos[5(\phi - \Psi_5)] + \dots$$



Anisotropic Flow at RHIC-LHC



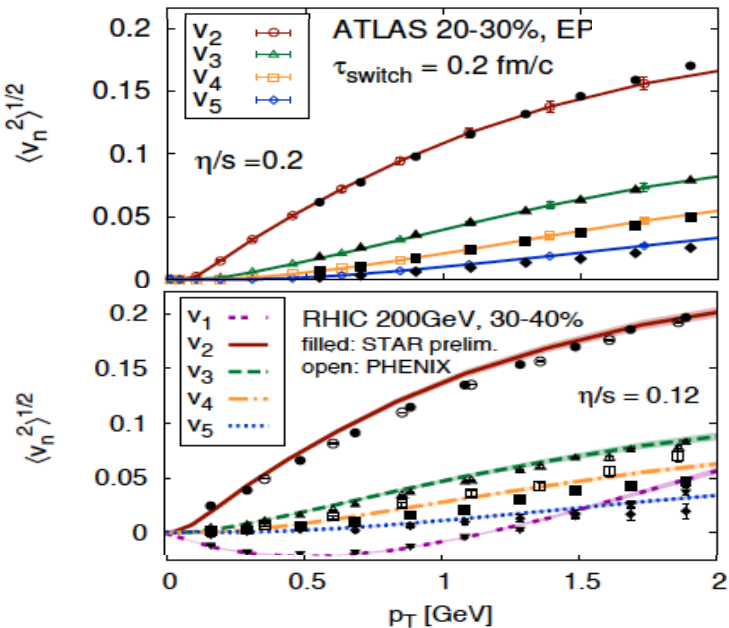
$$\epsilon_n = \sqrt{\frac{\langle r^n \cos n\phi \rangle + \langle r^n \sin n\phi \rangle}{\langle r^n \rangle}}$$



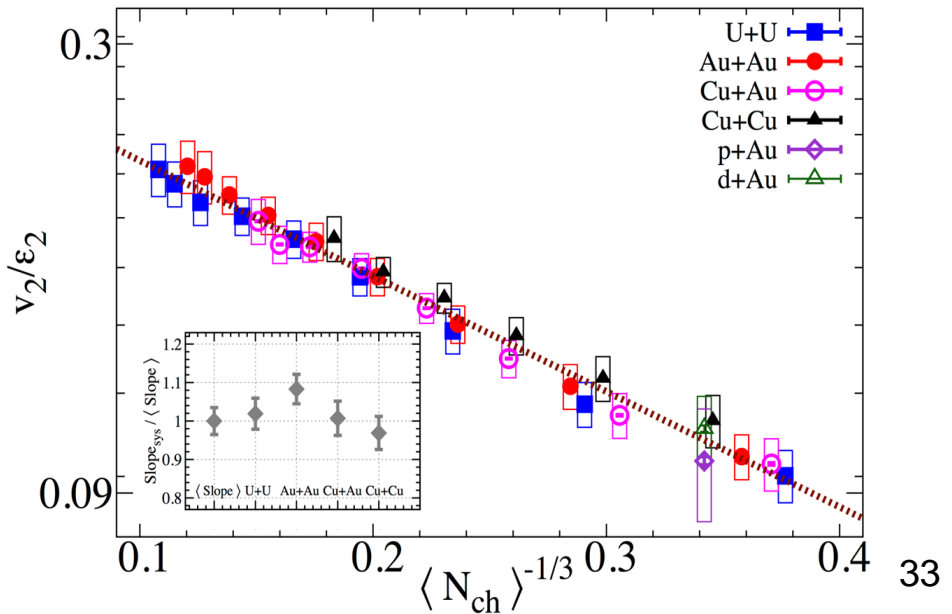
$$\frac{dN}{d\phi} \propto \left(1 + 2 \sum_{n=1} v_n \cos[n(\phi - \Psi_n)] \right)$$

Initial eccentricity (and its attendant fluctuations) ϵ_n drive momentum anisotropy v_n with specific viscous modulation

Gale, Jeon, et al., Phys. Rev. Lett. 110, 012302



Phys. Rev. Lett. 122 (2019) 172301



It's partons unchained?

Partonic degree of freedom at work ?

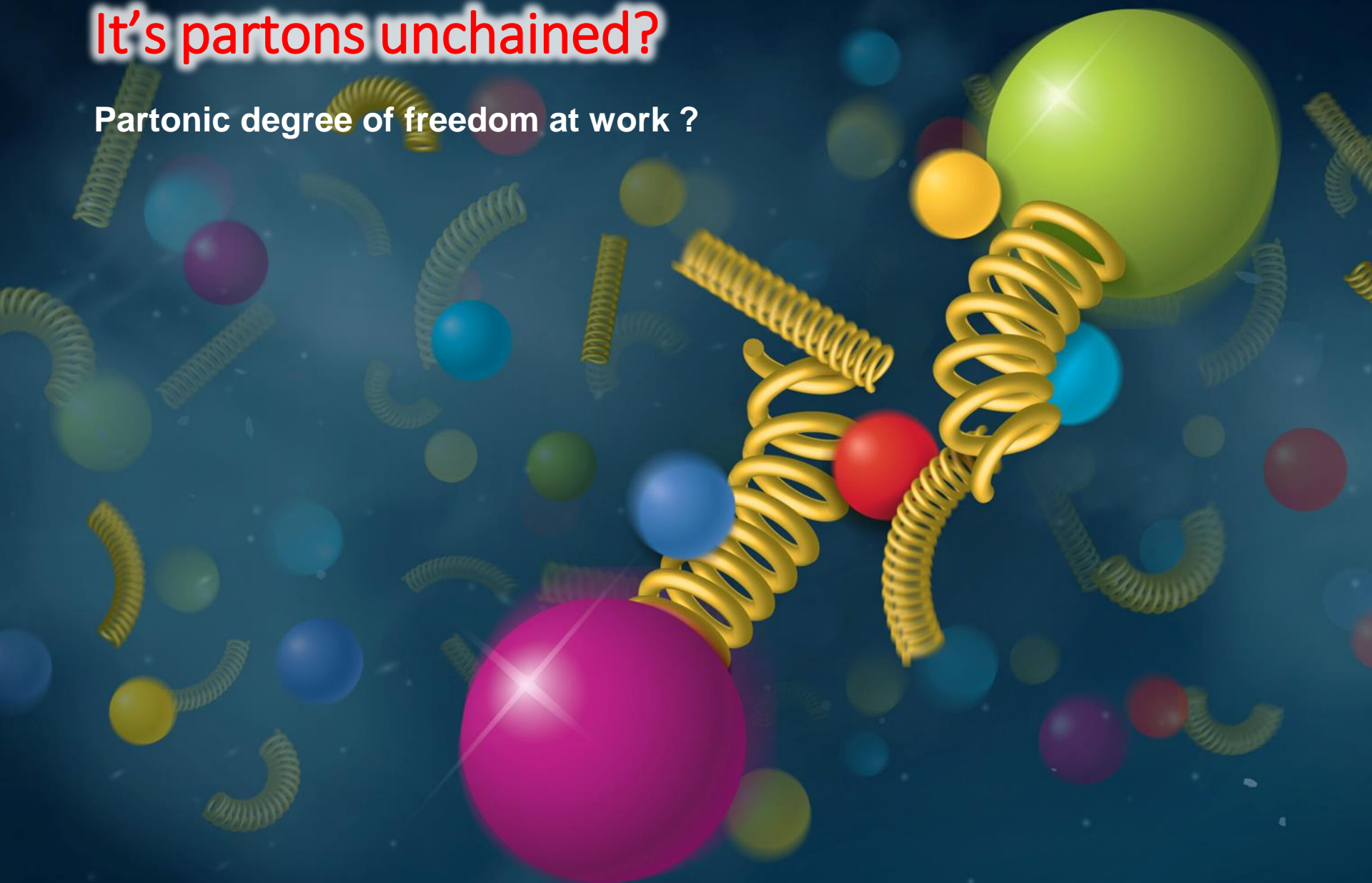
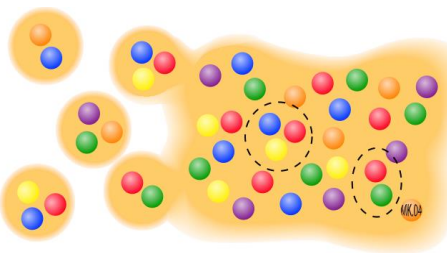
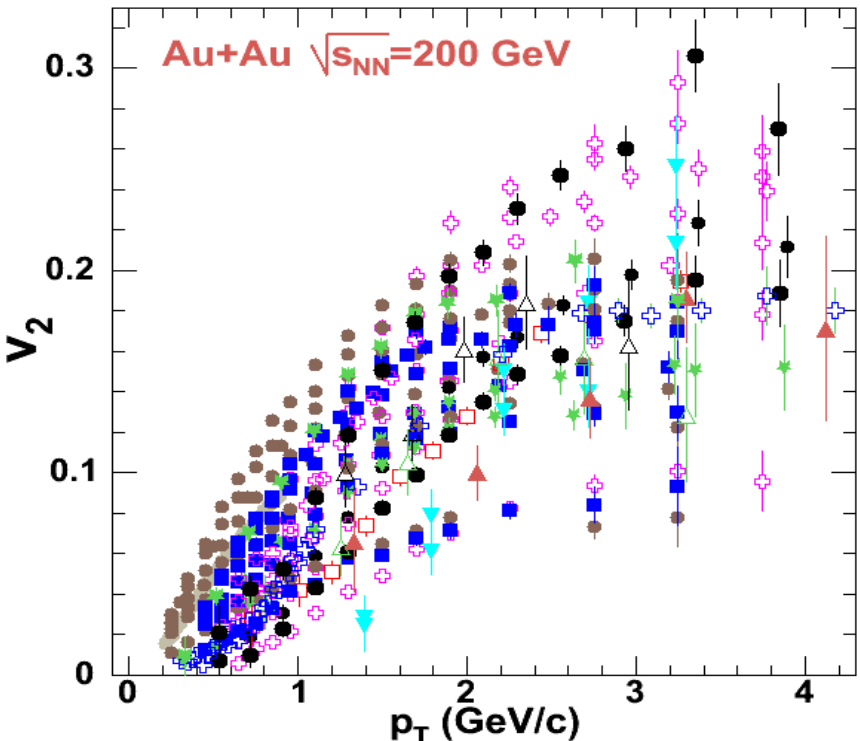


Image credit : BNL

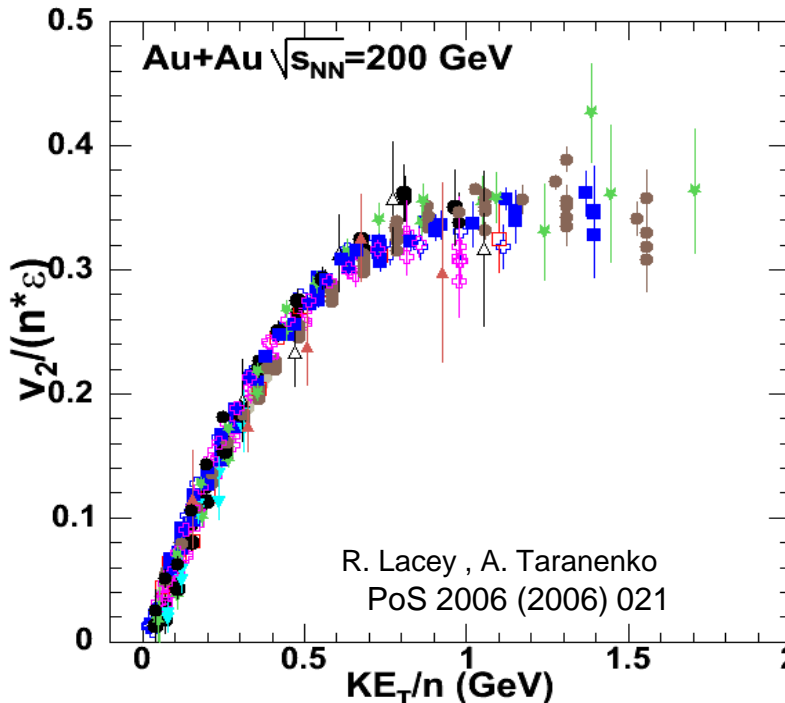
Anisotropic Flow at RHIC – partonic?



$n=2$ for mesons and
 $n=3$ for baryons

PHENIX (Phys.Rev.Lett.91, Preliminary: QM05, GRC 06)	
● - $\pi^+ + \pi^-$:	min.bias, 0-10%, 10-20%, 20-30%, 30-40%, 40-50%, 20-60%
■ - $K^+ + K^-$:	min.bias, 0-10%, 10-20%, 20-30%, 30-40%, 40-50%, 20-60%
✚ - $p + \bar{p}$:	min.bias, 0-10%, 10-20%, 20-30%, 30-40%, 40-50%, 20-60%
▼ - d :	min.bias, 10-50%
△ - ϕ :	20-60%
STAR (Phys. Rev. Lett. 92, Phys. Rev. C 72 (2005), Preliminary QM05, SQM06)	
● - $\pi^+ + \pi^-$:	min.bias
★ - $K_S^0 \pm$:	min.bias, 5-30%, 30-70%
✚ - $p + \bar{p}$:	min.bias
● - $\Lambda + \bar{\Lambda}$:	min.bias, 5-30%, 30-70%
□ - $\Xi + \bar{\Xi}$:	min.bias
▲ - $\Omega + \bar{\Omega}$:	min.bias
△ - ϕ :	min.bias

$$KE_T = m (\gamma_T - 1) = m_T - m$$



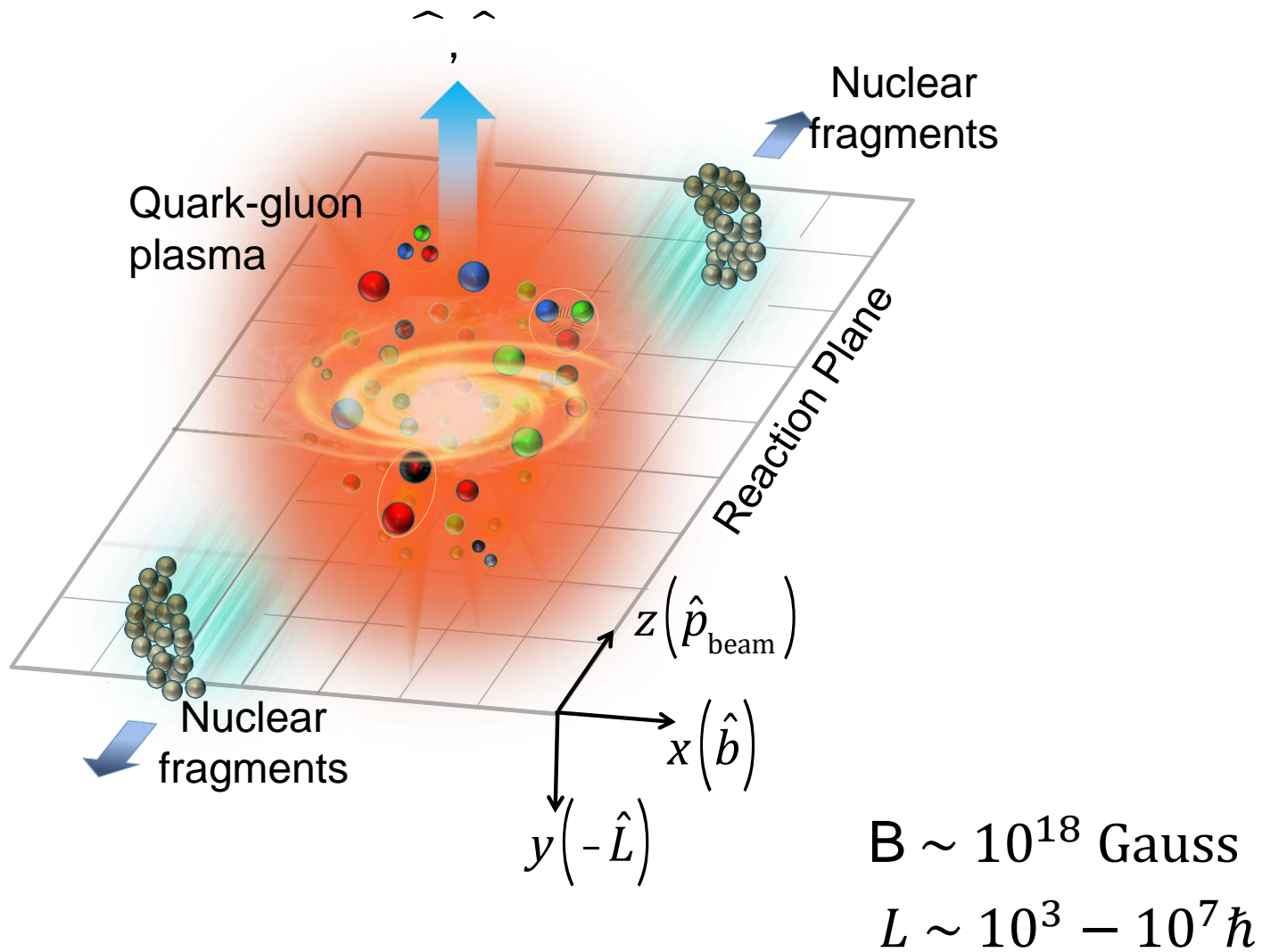
The background features a dynamic, swirling pattern of translucent, colorful bands in shades of blue, red, green, and yellow. Interspersed within these bands are several small, glowing spheres in various colors like red, blue, green, and white. The overall effect is one of motion and energy.

It's swirling fast

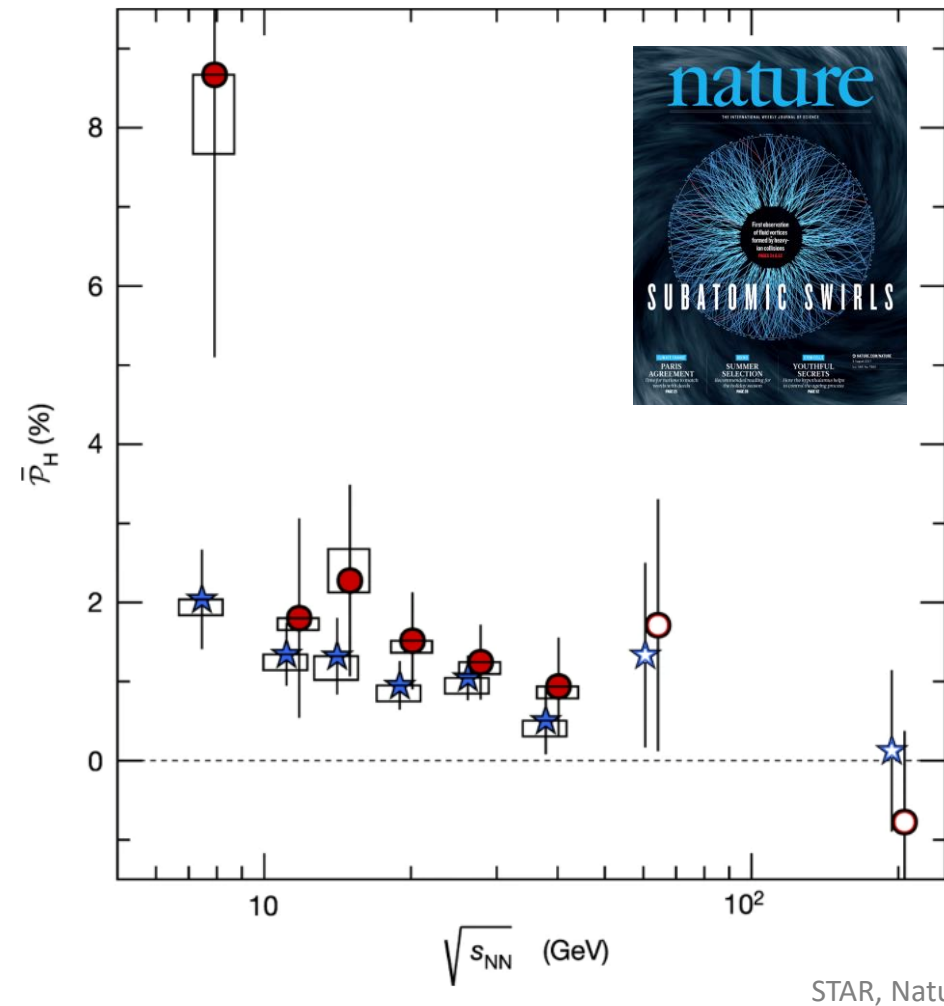
Most vortical fluid !

Image credit : BNL

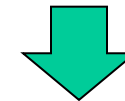
QGP Under Rotation



Λ Global Polarization



$$P_\Lambda \approx \frac{1}{2} \frac{\omega}{T} + \frac{\mu_\Lambda B}{T} \quad P_{\bar{\Lambda}} \approx \frac{1}{2} \frac{\omega}{T} - \frac{\mu_\Lambda B}{T}$$



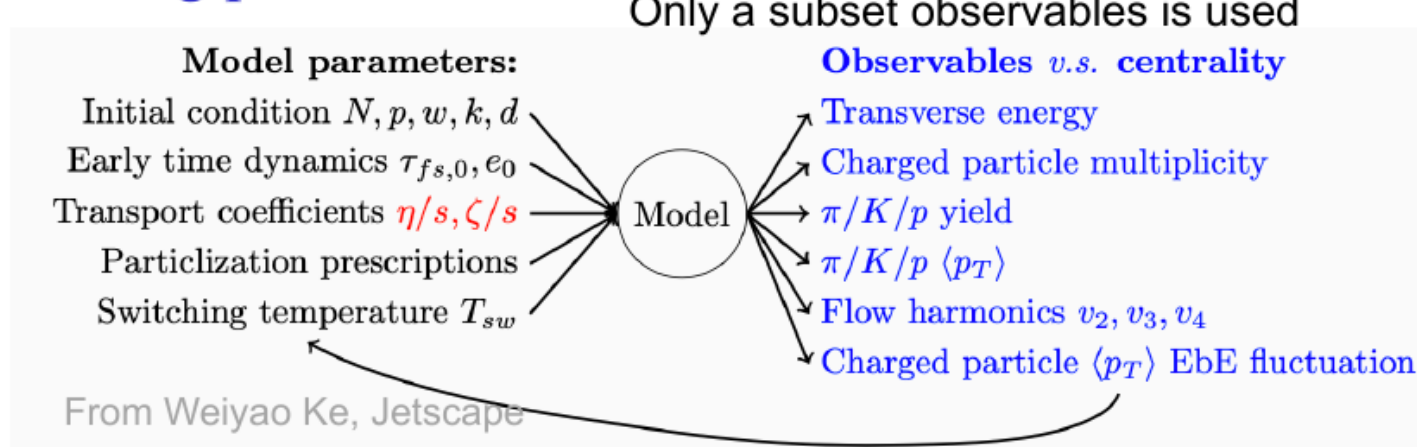
$$\omega = (P_\Lambda + P_{\bar{\Lambda}})k_B T / \hbar \sim 10^{22} s^{-1}$$

RHIC : $\omega \sim 10^{22} s^{-1}$
Most vortical fluid !

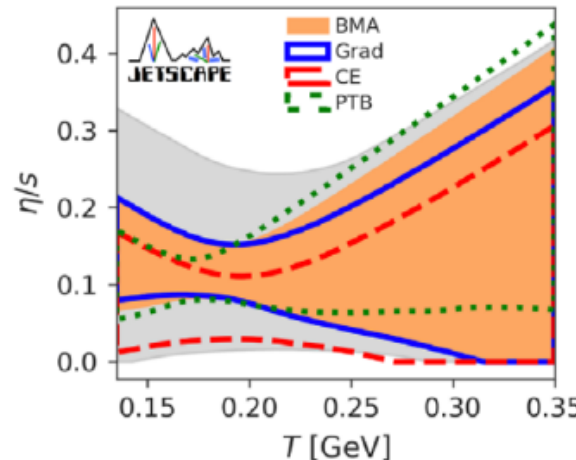
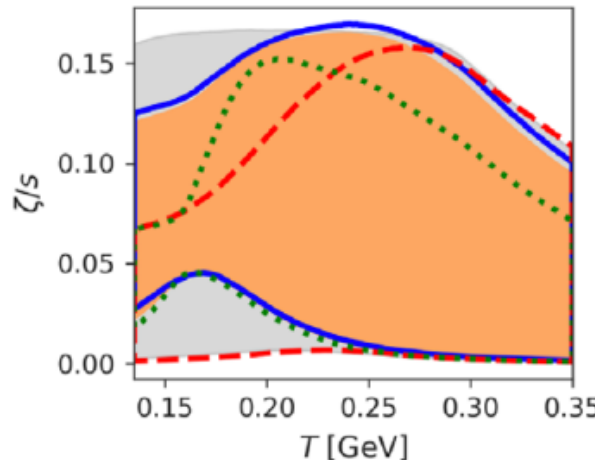
State-of-the-art modeling of HI collisions

8

- Data-model comparison via Bayesian inference to optimize constraining power.



- Detailed temperature dependence of viscosity!



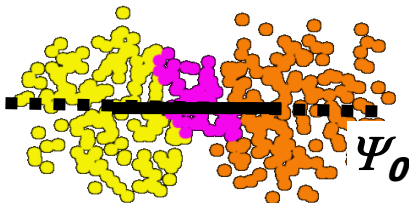
Jetscape PRL.126.242301
Trjactum PRL.126.202301

Major uncertainty: initial condition and pre-hydro phase

System size scan at top RHIC energy ($\sqrt{s_{NN}} = 200$ GeV)

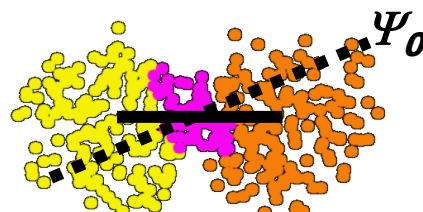
2001-2005

$$\varepsilon_{\text{std}} = \frac{\sigma_y^2 - \sigma_x^2}{\sigma_x^2 + \sigma_y^2}$$



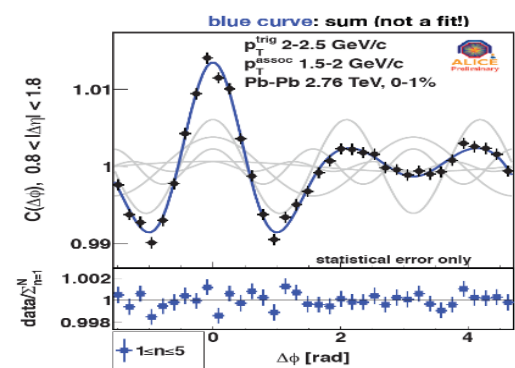
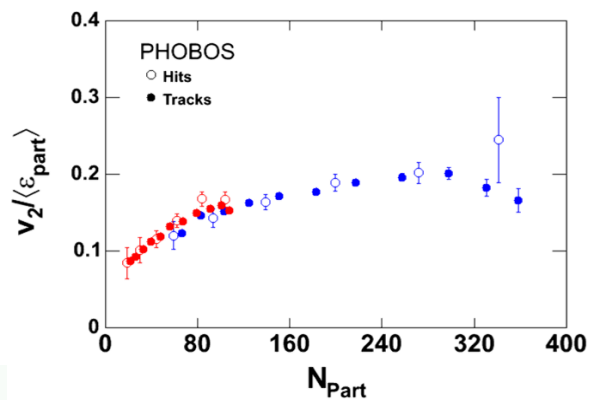
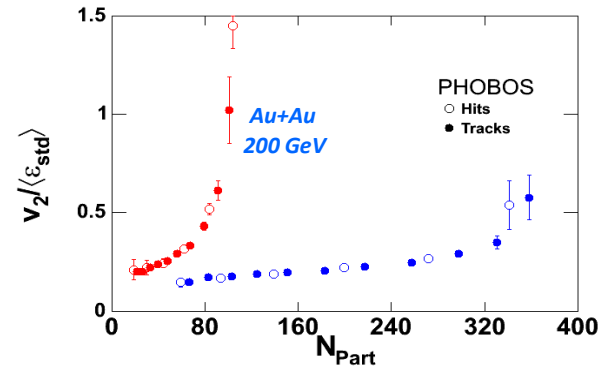
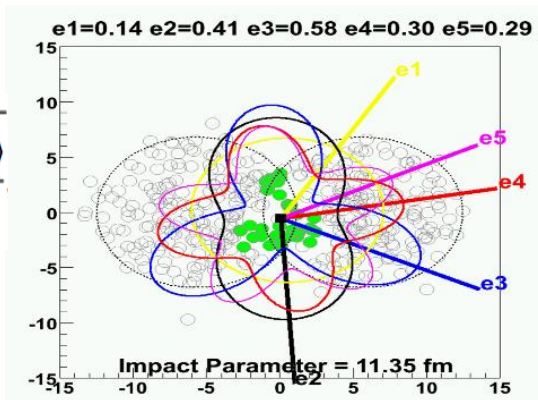
2005-2011

$$\langle \epsilon_{\text{part}} \rangle = \frac{(\sigma_y^2 - \sigma_x^2)^2 + 4\sigma_{xy}^2}{(\sigma_y^2 + \sigma_x^2)}$$

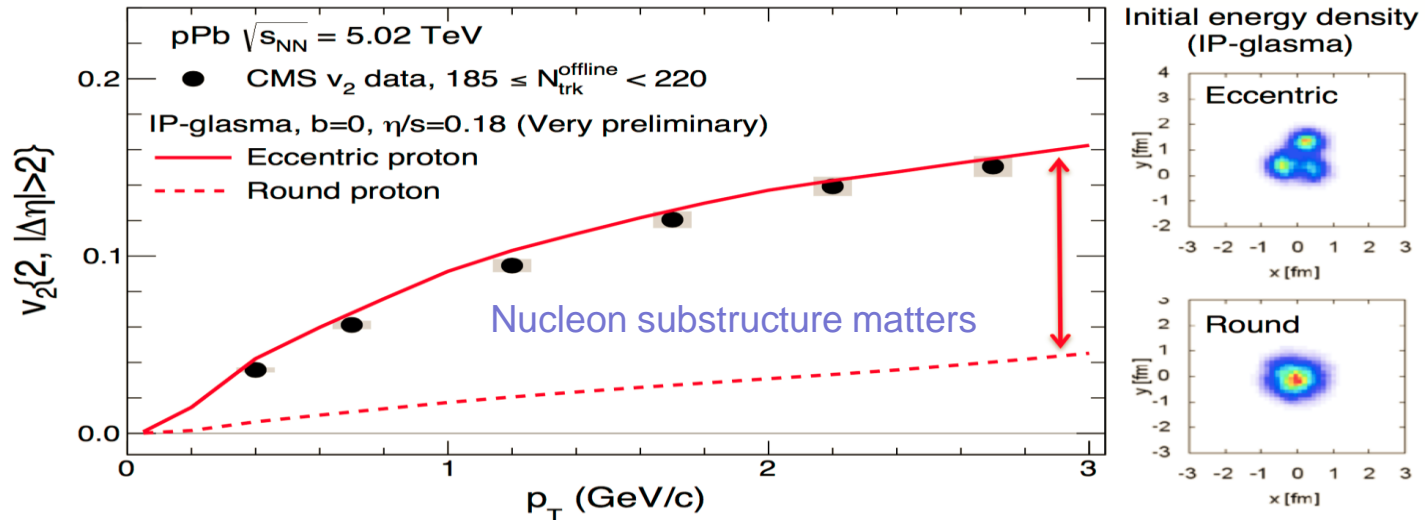


2011-2012

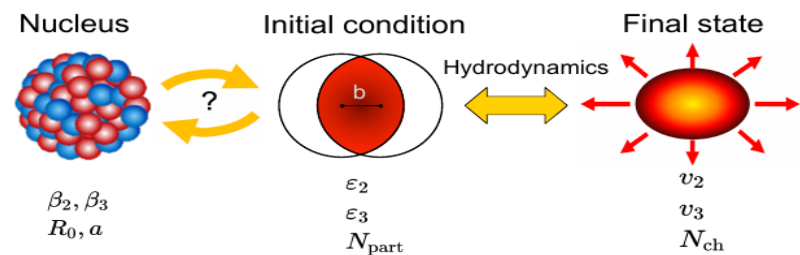
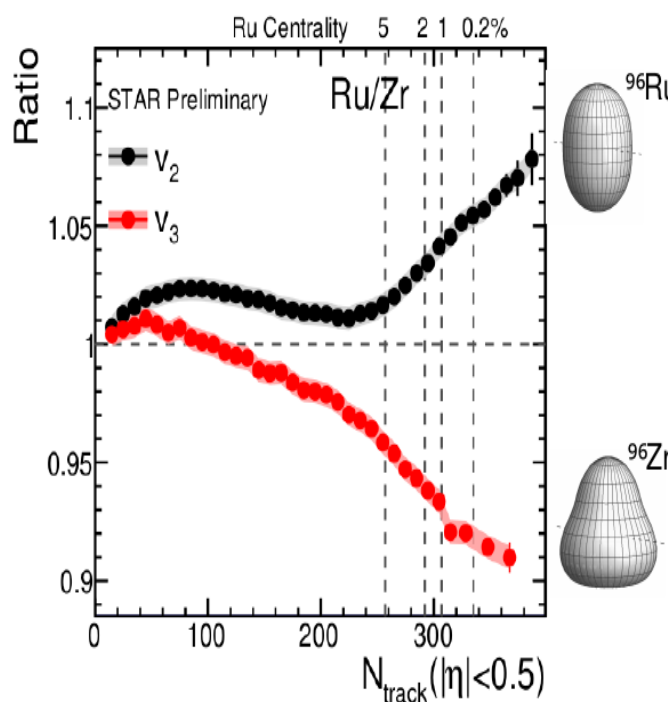
$$\epsilon_n = \sqrt{\frac{\langle r^n \cos n\phi \rangle + \langle r^n \sin n\phi \rangle}{\langle r^n \rangle}}$$



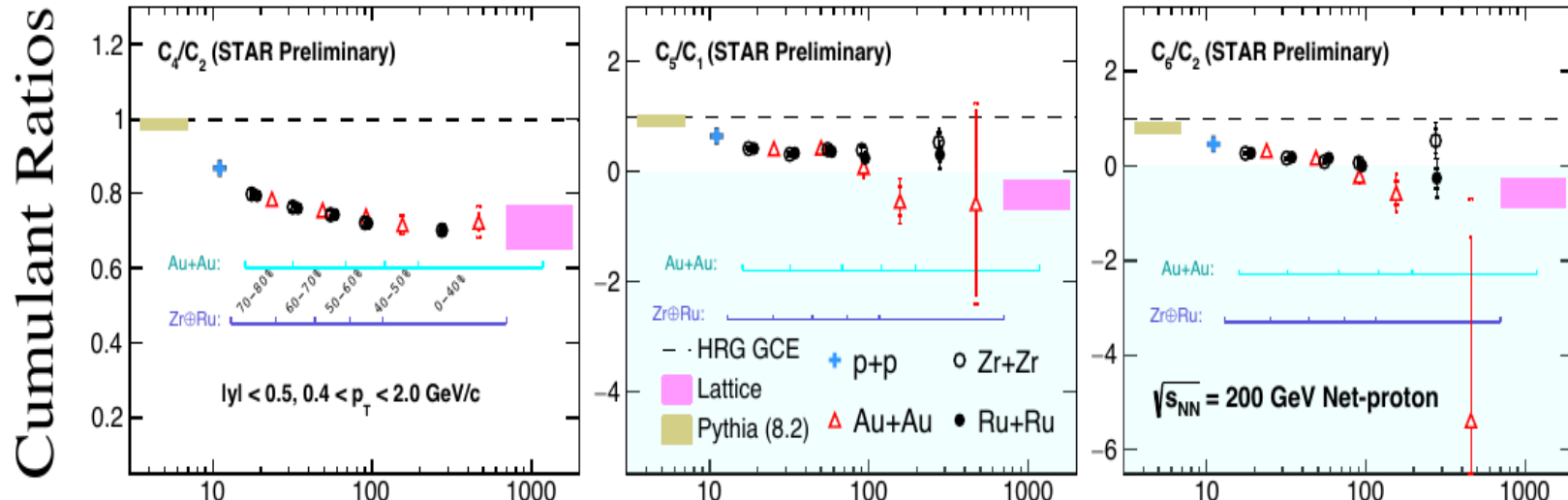
2011-2016



2020-2022



Net-p in 200 GeV p+p and Au+Au Collisions



STAR: CPOD2021,
SQM2021, QM2022

Charged Particle Multiplicity

- 1) In 200GeV p+p collisions, high order cumulants ratios of net-protons are found to be positive for: C_4/C_2 , C_5/C_2 and C_6/C_2 ;
- 2) For QGP matter, LGT predicted negative net-baryon C_5/C_2 and C_6/C_2 ;
- 3) Direct evidence for the QGP formation in 200GeV Au+Au central collisions!**

HotQCD Collaboration, PRD101, 074502 (2020)

LQCD \leftrightarrow Experiment

≡ Google Translate

Detect language

English German Spanish

LQCD

$$\chi_{klmn}^{BQSC} = \left. \frac{\partial^{(k+l+m+n)} [P(\hat{\mu}_B, \hat{\mu}_Q, \hat{\mu}_S, \hat{\mu}_C) / T^4]}{\partial \hat{\mu}_B^k \partial \hat{\mu}_Q^l \partial \hat{\mu}_S^m \partial \hat{\mu}_C^n} \right|_{\hat{\mu}=0}$$



Baryon number (**B**), Strangeness (**S**), Electric charge (**Q**), Cham (**C**)

0 / 5,000

↔ **EXPERIMENT**

Spanish



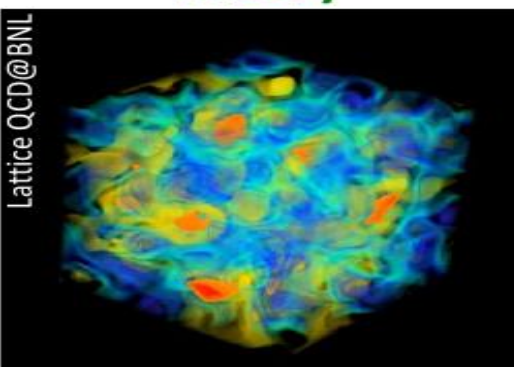
Translation

$$\chi_2^B = \frac{\kappa_2(\Delta N_B)}{V T^3} \rightarrow \frac{\kappa_4(\Delta N_B)}{\kappa_2(\Delta N_B)} = \frac{\chi_4^B}{\chi_2^B}$$

κ_n → cumulants of $\Delta N_B = N_B - N_{\bar{B}}$

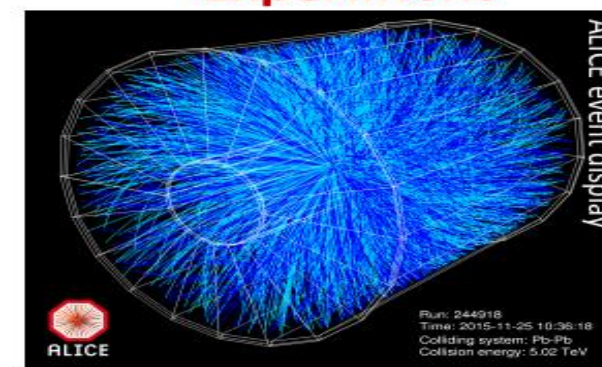
Bridge experimental data to LQCD calculations

Lattice QCD@BNL



Theory

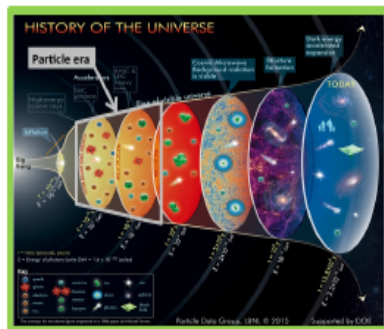
Experiment



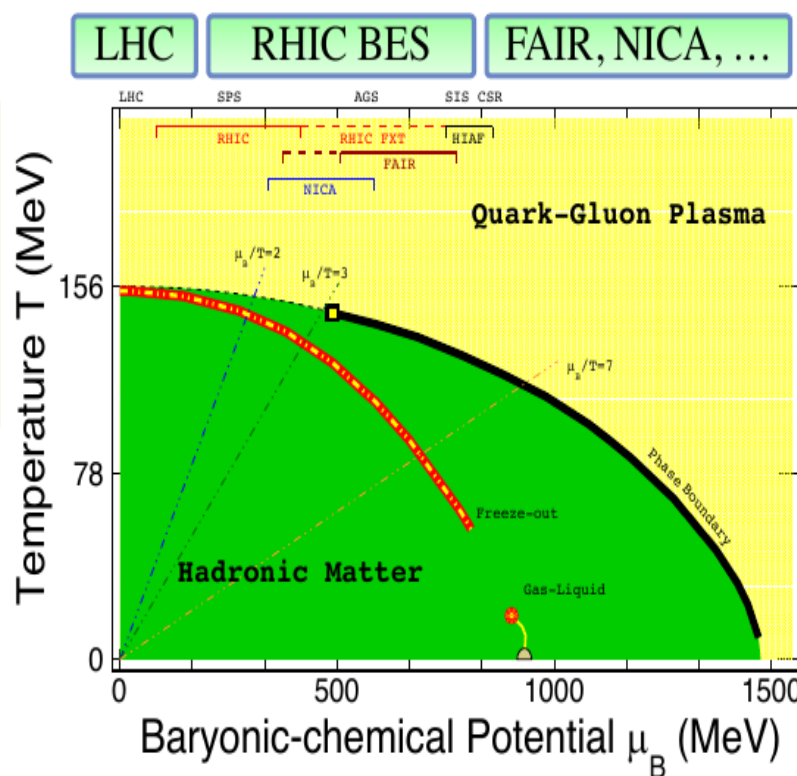
Static	Dynamic
Coordinate space	Momentum space
Net-baryon	Net-proton
Fixed V	Fluctuating V
...	...

- **Experimental challenges:** Particle identification, efficiency correction, effect of event pileup, volume fluctuations ...
- **Theoretical/phenomenological challenges:** Effect of resonances, charge conservation, effect of magnetic field, cluster formation, baryon annihilation, excluded volume ...

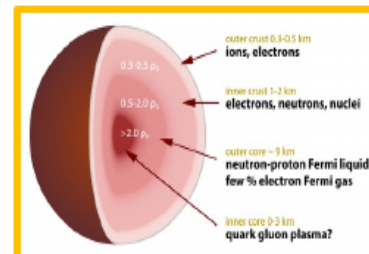
Relativistic Heavy-Ion Collisions and QCD Phase Diagram



High temperature:
Early Universe evolution

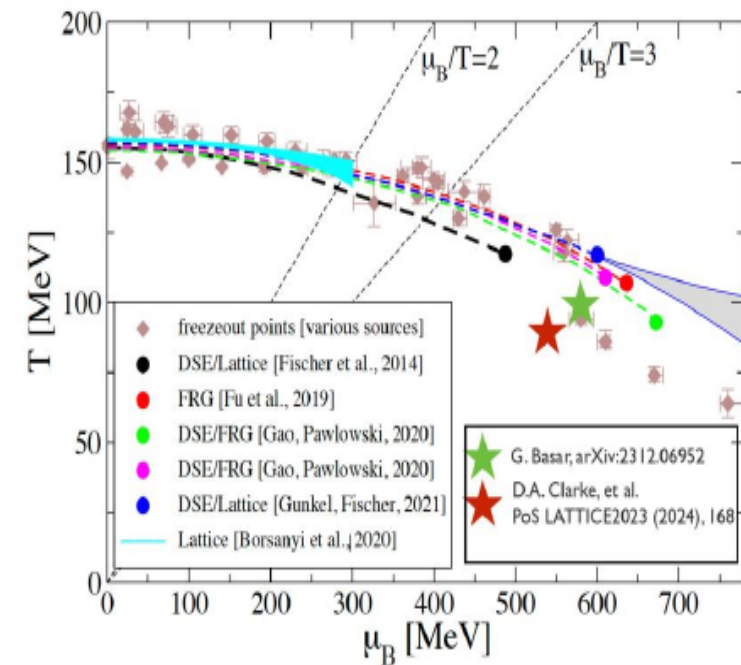
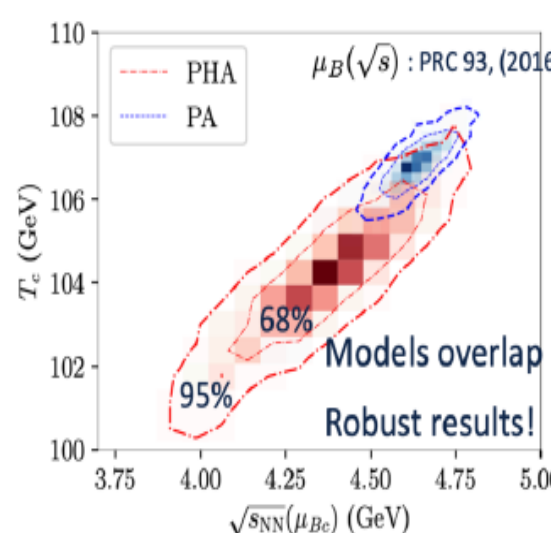
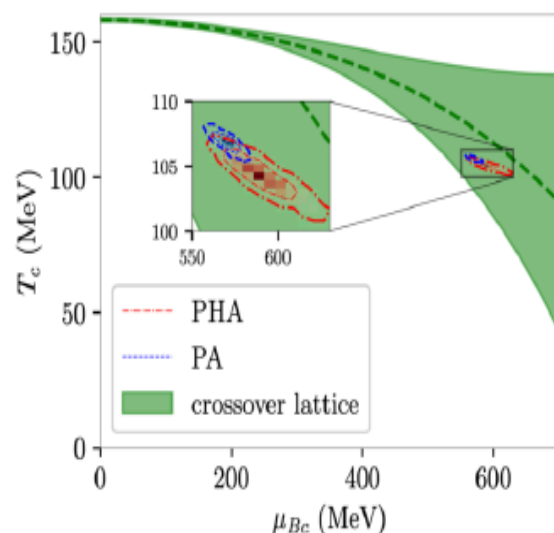


High baryon density:
Inner structure of
compact stars



- 1) At $\mu_B = 0$, smooth crossover (LGT + data) ;
- 2) Large μ_B , 1st order phase transition → **QCD critical point**

Location of the QCD Critical Point : Theoretical Estimation/Prediction



Holography+ Bayesian : Hippert et al., arXiv : 2309.00579

CPOD2024

Method	μ_c (MeV)	T_c (MeV)
Holography + Bayesian	560 - 625	101 - 108
FRG/DSE	495 - 654	108 - 119
Lee-Yang edge singularities	500 - 600	100 - 105
Lattice QCD	$\mu_c/T_c > 3$	F. Karsch et al.
Summary	495 - 654	100 - 119

$$(\mu_c, T_c) = (495 - 654, 100 - 119) \text{ MeV} \rightarrow 3.5 < \sqrt{s_{NN}} < 4.9 \text{ GeV}$$

STAR BES-I and BES-II Data Sets

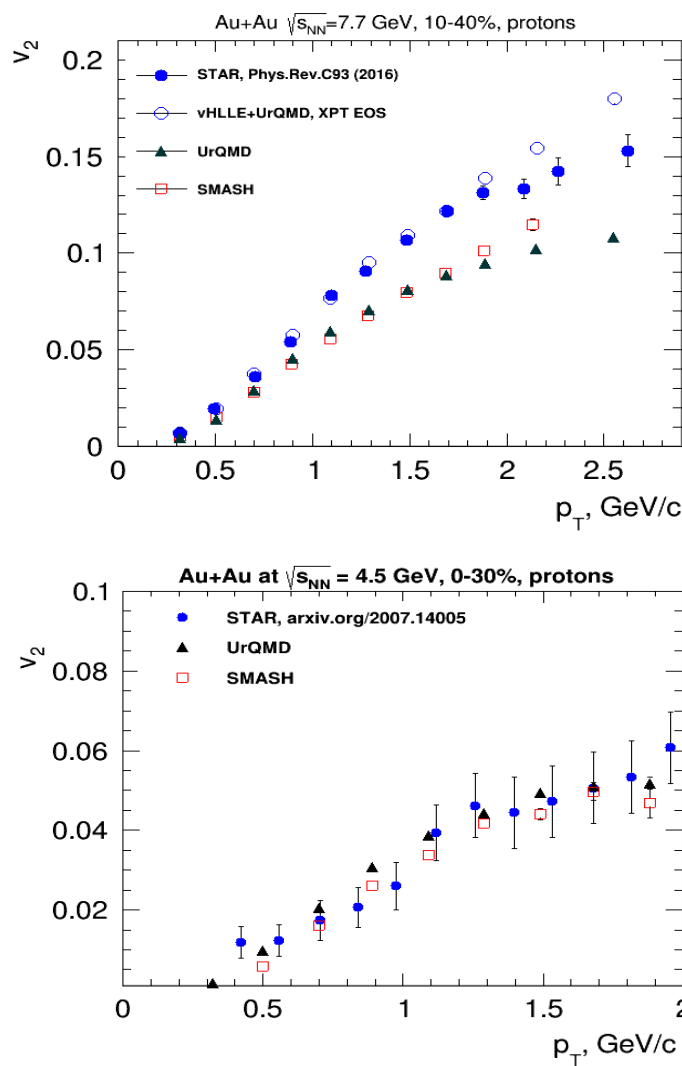
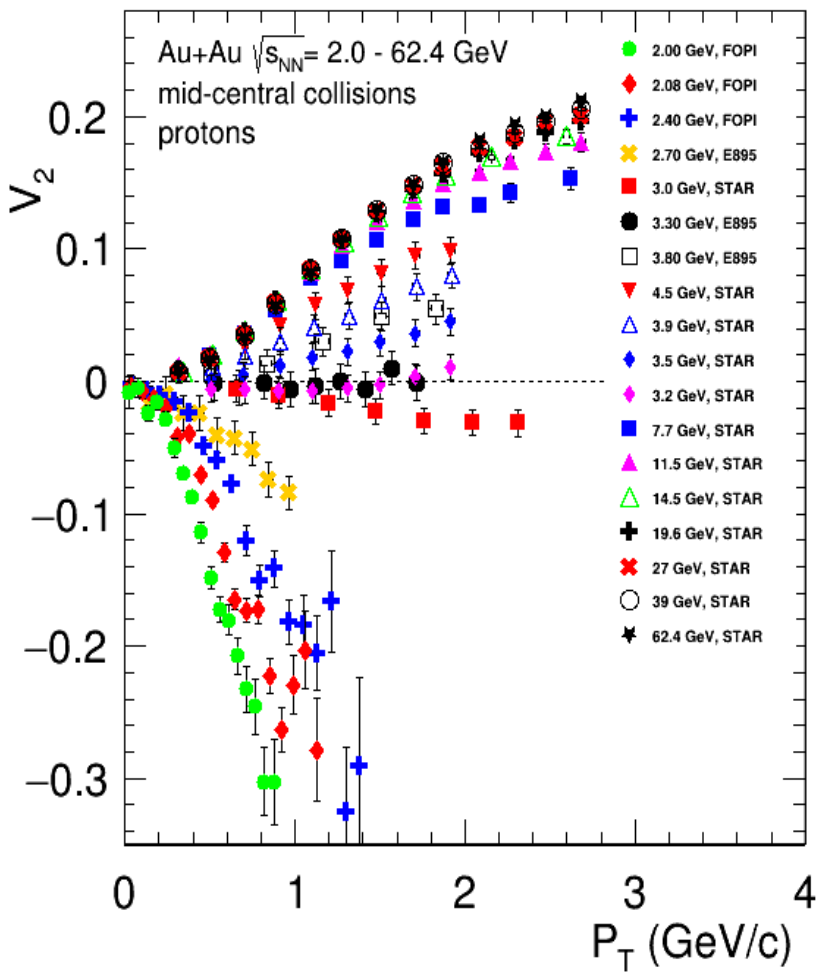
Au+Au Collisions at RHIC

Collider Runs						Fixed-Target Runs					
	$\sqrt{s_{NN}}$ (GeV)	#Events	μ_B	y_{beam}	run		$\sqrt{s_{NN}}$ (GeV)	#Events	μ_B	y_{beam}	run
1	200	380 M	25 MeV	5.3	Run-10, 19	1	13.7 (100)	50 M	280 MeV	-2.69	Run-21
2	62.4	46 M	75 MeV		Run-10	2	11.5 (70)	50 M	320 MeV	-2.51	Run-21
3	54.4	1200 M	85 MeV		Run-17	3	9.2 (44.5)	50 M	370 MeV	-2.28	Run-21
4	39	86 M	112 MeV		Run-10	4	7.7 (31.2)	260 M	420 MeV	-2.1	Run-18, 19, 20
5	27	585 M	156 MeV	3.36	Run-11, 18	5	7.2 (26.5)	470 M	440 MeV	-2.02	Run-18, 20
6	19.6	595 M	206 MeV	3.1	Run-11, 19	6	6.2 (19.5)	120 M	490 MeV	1.87	Run-20
7	17.3	256 M	230 MeV		Run-21	7	5.2 (13.5)	100 M	540 MeV	-1.68	Run-20
8	14.6	340 M	262 MeV		Run-14, 19	8	4.5 (9.8)	110 M	590 MeV	-1.52	Run-20
9	11.5	157 M	316 MeV		Run-10, 20	9	3.9 (7.3)	120 M	633 MeV	-1.37	Run-20
10	9.2	160 M	372 MeV		Run-10, 20	10	3.5 (5.75)	120 M	670 MeV	-1.2	Run-20
11	7.7	104 M	420 MeV		Run-21	11	3.2 (4.59)	200 M	699 MeV	-1.13	Run-19
						12	3.0 (3.85)	2000 M	750 MeV	-1.05	Run-18, 21

Precision data to map the QCD phase diagram

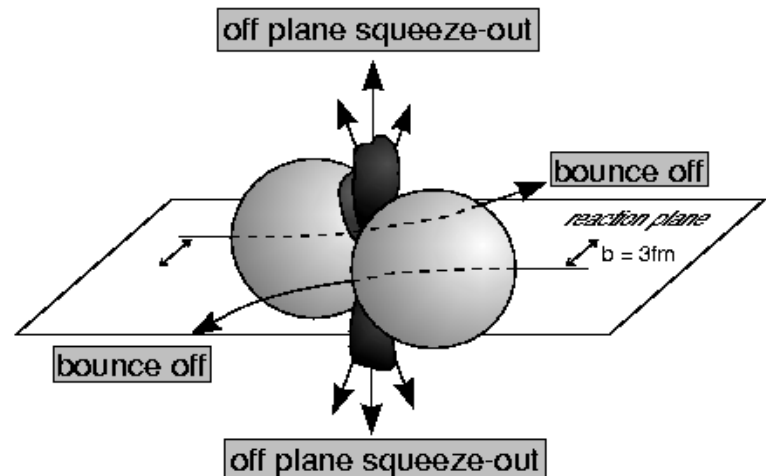
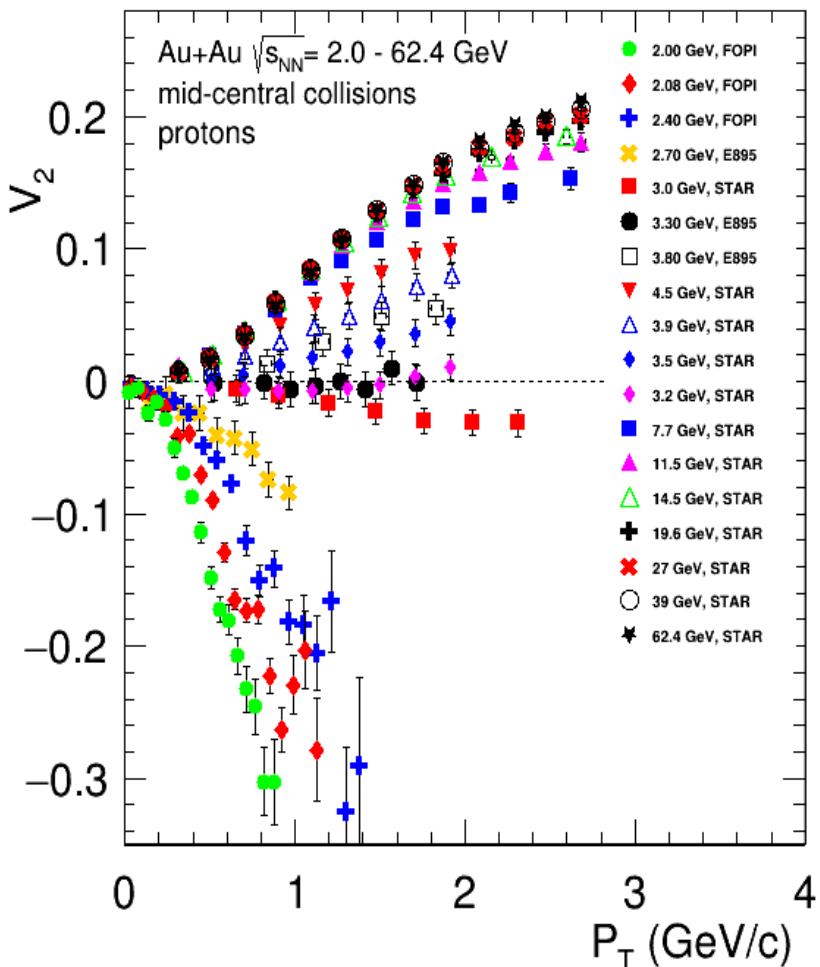
$3 < \sqrt{s_{NN}} < 200$ GeV; $750 < \mu_B < 25$ MeV

Beam Energy Dependence of Elliptic Flow (v_2)



- Strong energy dependence of v_2 at $\sqrt{s_{NN}} = 3-11$ GeV
 - ▶ $v_2 \approx 0$ at $\sqrt{s_{NN}} = 3.3$ GeV and negative below

Beam Energy Dependence of Elliptic Flow (v_2)

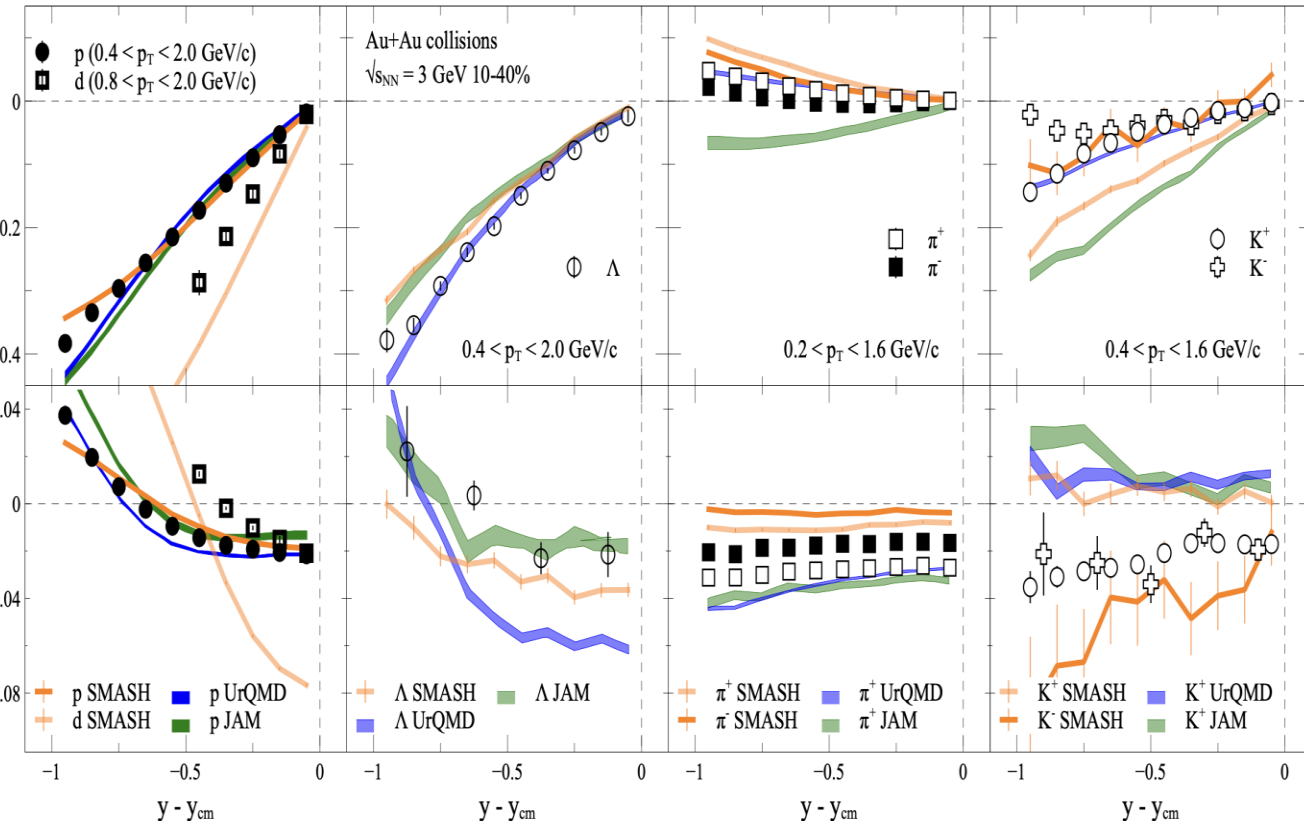


Passage time: $2R/(\beta_{cm}v_{cm})$

Expansion time: R/c_s $c_s = c\sqrt{dp/d\varepsilon}$ - speed of sound

$v_{1,2}(y)$ in Au+Au $\sqrt{s_{NN}}=3$ GeV: models vs. STAR data

A. Sorensen et. al., Prog.Part.Nucl.Phys. 134 (2024) 104080



Model description of v_n :

- Good overall agreement for v_n of protons
- v_n of light nuclei is not described
- v_n of Λ is not well described
 - nucleon-hyperon and hyperon-hyperon interactions
- Light mesons (π, K) are not described
 - No mean-field for mesons

Models have a huge room for improvement in terms of describing v_n

EOS for high baryon density matter

The binding energy per nucleon: $E_A(\rho, \delta) = E_A(\rho, 0) + E_{sym}(\rho)\delta^2 + O(\delta^4)$

Isospin asymmetry:

$$\delta = (\rho_n - \rho_p)/\rho$$

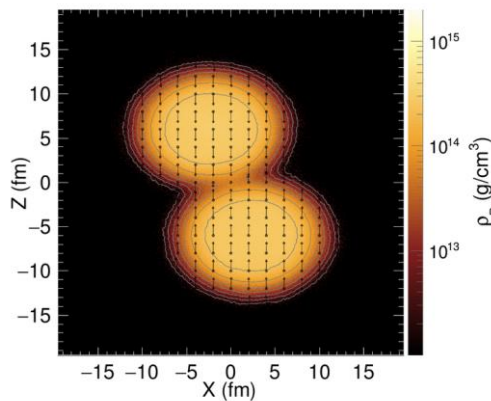
Symmetric matter

Symmetry energy

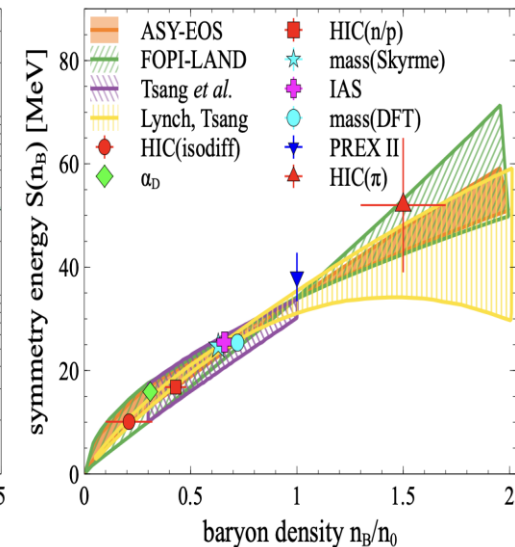
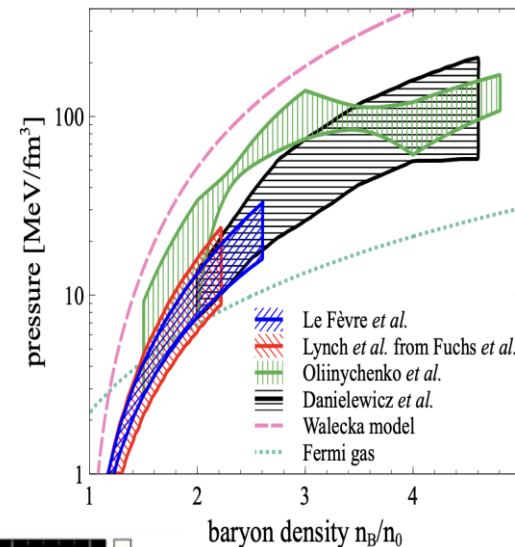
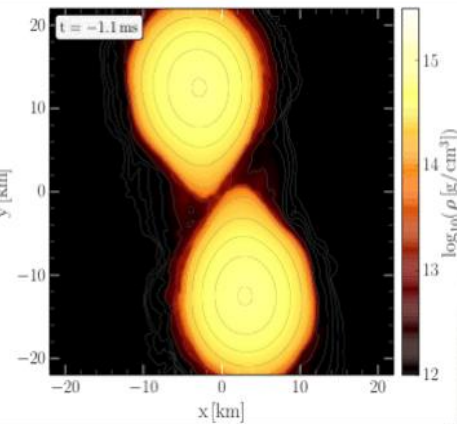
Heavy-Ion Collisions and Merging Neutron Stars

- $T < 70$ MeV, $\rho \approx 3\rho_0$ for both
- Probe NS merger matter in the laboratory

Au+Au 1.25A GeV



NS mergers

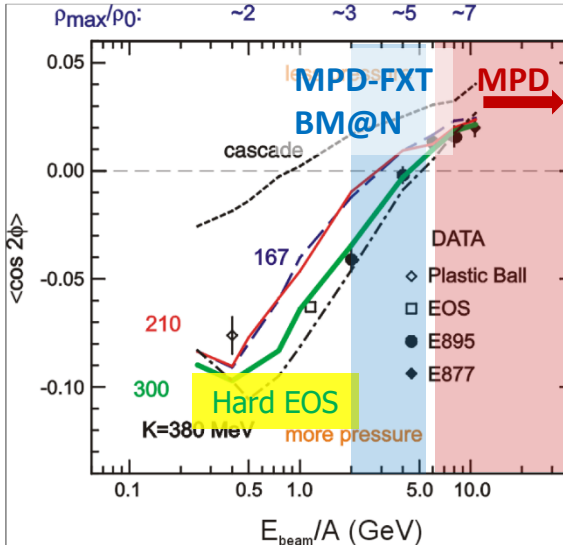
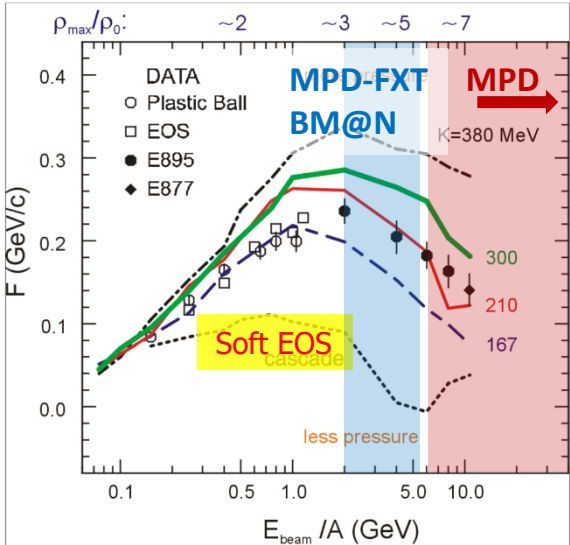


A. Sorensen et. al., Prog.Part.Nucl.Phys. 134 (2024) 104080

New data is needed to further constrain transport models with hadronic d.o.f.

Sensitivity of the collective flow to the EOS

P. Danielewicz, R. Lacey, W.G. Lynch, Science 298 (2002) 1592



$$F = \frac{d\langle p_x/A \rangle}{d(y/y_{cm})} \Big|_{y/y_{cm}=1}$$

$$\nu_2 \equiv \langle \cos(2(\varphi - \Psi_{RP})) \rangle$$

Mean field usually can be defined using Skyrme potential with:

$$U(n_B) = A \left(\frac{n_B}{n_0} \right) + B \left(\frac{n_B}{n_0} \right)^{\tau}$$

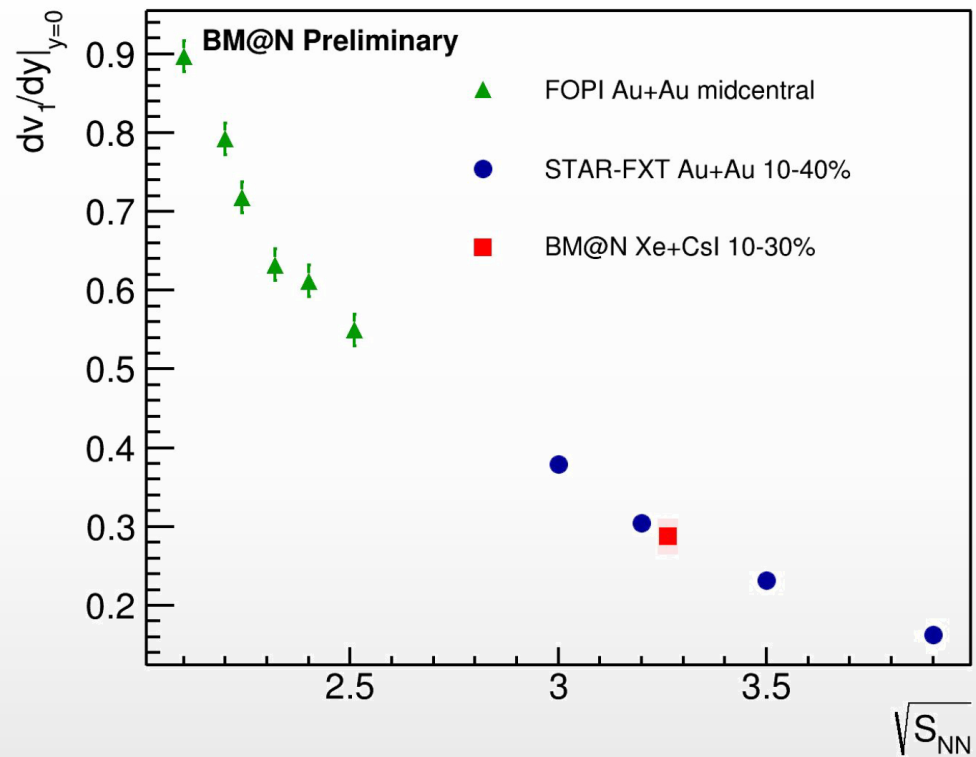
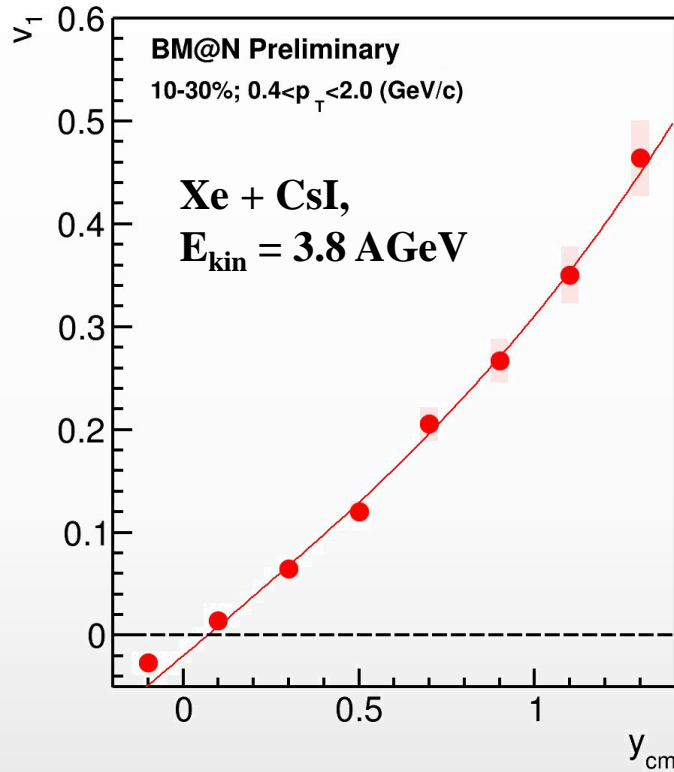
Discrepancy in the interpretation:

- ν_1 suggests soft EoS
- ν_2 suggests hard EoS

New measurements using new data and modern analysis techniques will address this discrepancy

More detailed model study should be done to address n_B -dependence of incompressibility K_0

Additional measurements are essential to clarify the previous measurements



- ❖ Slope of v_1 is in good agreement with the world data
See Mikhail Mamaev talk at AYSS2024

MPD physics program

G. Feofilov, P. Parfenov

Global observables

- Total event multiplicity
- Total event energy
- Centrality determination
- Total cross-section measurement
- Event plane measurement at all rapidities
- Spectator measurement

V. Kolesnikov, Xianglei Zhu

Spectra of light flavor and hypernuclei

- Light flavor spectra
- Hyperons and hypernuclei
- Total particle yields and yield ratios
- Kinematic and chemical properties of the event
- Mapping QCD Phase Diag.

K. Mikhailov, A. Taranenko

Correlations and Fluctuations

- Collective flow for hadrons
- Vorticity, Λ polarization
- E-by-E fluctuation of multiplicity, momentum and conserved quantities
- Femtoscopy
- Forward-Backward corr.
- Jet-like correlations

D. Peresunko, Chi Yang

Electromagnetic probes

- Electromagnetic calorimeter meas.
- Photons in ECAL and central barrel
- Low mass dilepton spectra in-medium modification of resonances and intermediate mass region

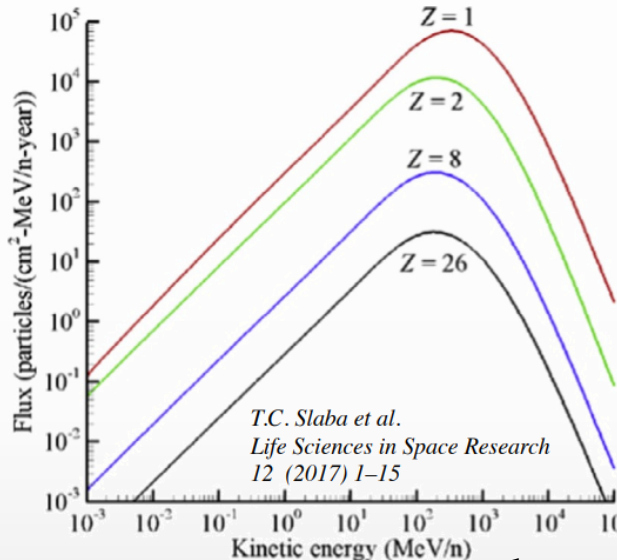
Wangmei Zha, A. Zinchenko

Heavy flavor

- Study of open charm production
- Charmonium with ECAL and central barrel
- Charmed meson through secondary vertices in ITS and HF electrons
- Explore production at charm threshold

High-energy heavy-ion reaction data

- ❖ Galactic Cosmic Rays composed of nuclei (protons, ... up to Fe) and E/A up to 50 GeV
- ❖ These high-energy particles create cascades of hundreds of secondary, etc. particles



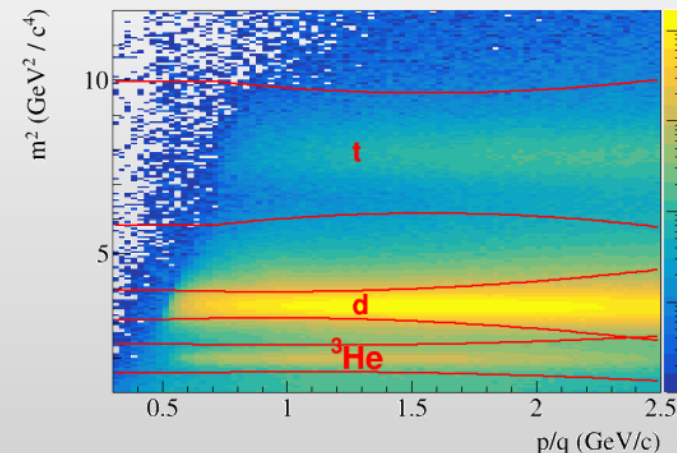
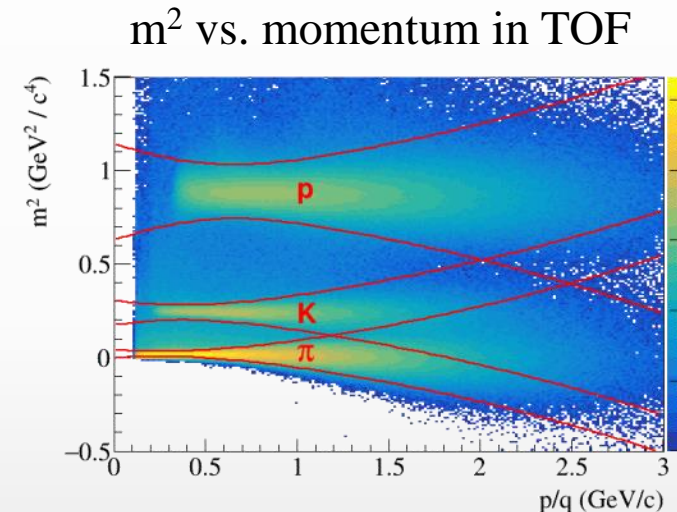
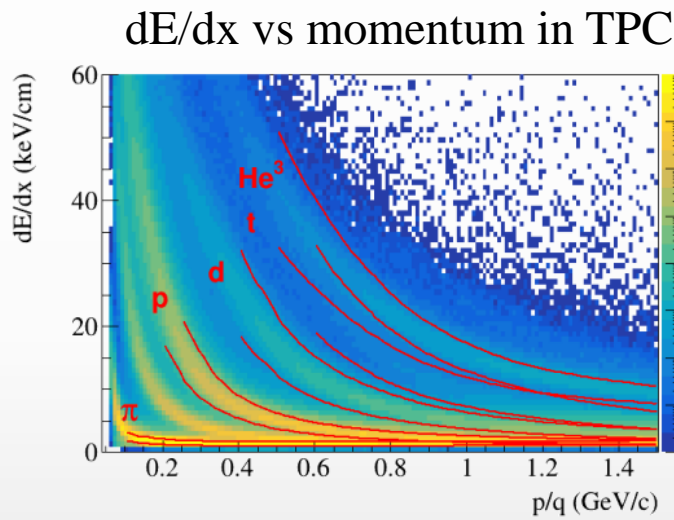
T.C. Slaba et al.
Life Sciences in Space Research
12 (2017) 1–15

- ❖ Cosmic rays are a serious concern to astronauts, electronics, and spacecraft.
- ❖ The damage is proportional to Z^2 , therefore the component due to ions is important
- ❖ Damage from secondary production of p, d, t, ${}^3\text{He}$, and ${}^4\text{He}$ is also significant
- ❖ Need input information for transport codes for shielding applications (Geant-4, Fluka, PHITS, etc.):

- ✓ total, elastic/reaction cross section
- ✓ particle multiplicities and coellicense parameters
- ✓ outgoing particle distributions: $d^2N/dEd\Omega$

High energy heavy ion reaction data

- ❖ NICA can deliver different ion beam species and energies:
 - ✓ Targets of interest (C = astronaut, Si = electronics, Al = spacecraft) + He, C, O, Si, Fe, etc.
- ❖ No data exist for projectile energies $> 3 \text{ GeV/n}$



MPD has excellent light fragment identification capabilities in a wide rapidity range → unique capability of the MPD in the NICA energy range

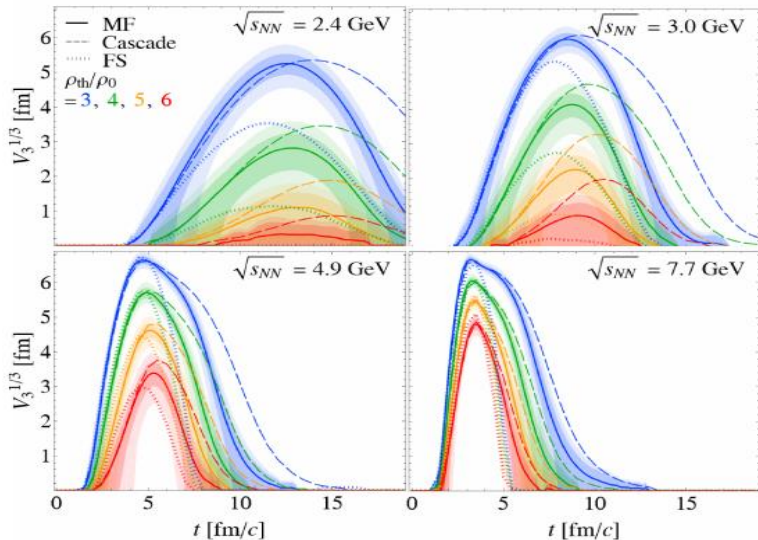
Summary



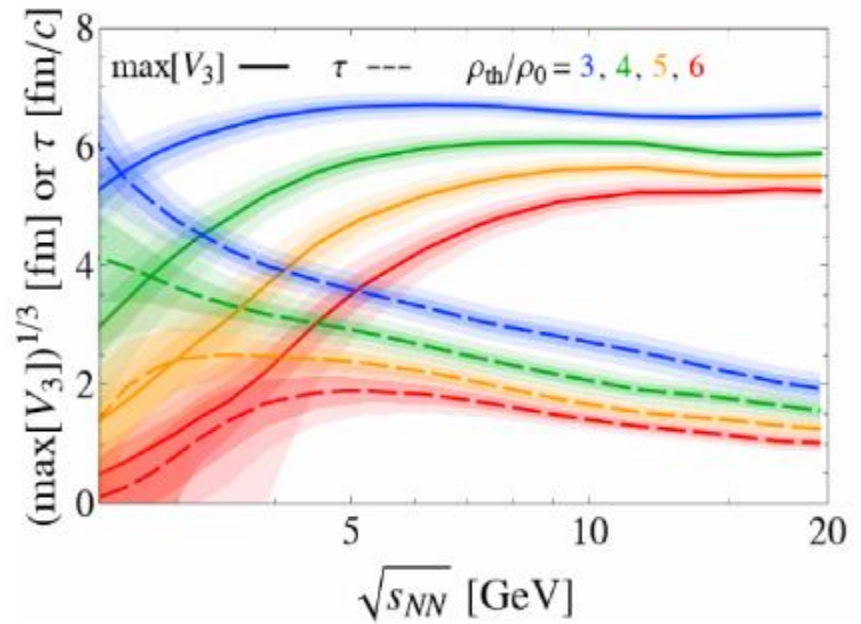
- ❖ NICA open unique opportunities for the exploration of the properties of dense nuclear matter.
Complementary energy range, large discovery potential.
- ❖ Preparation of the MPD detector and experimental program is ongoing, all activities are continued
- ❖ All components of the MPD 1-st stage detector are in advanced state of production
- ❖ Commissioning of the MPD Stage-I detector is expected in 2025-2026
- ❖ BM@N **first physics run with Xe+CsI - finished – good data**
- ❖ Further program will be driven by the physics demands and NICA capabilities

Optimal collision energy for realizing high baryon-density matter

H. Taya, A. Jinno, M. Kitazawa, Y. Nara <https://arxiv.org/abs/2409.07685>



Dense region disappears more quickly for larger $\sqrt{s_{NN}}$



$\sqrt{s_{NN}}$ dependence of the maximum volume $\max[V_3]$ (solid) and the lifetime τ (dashed)

The optimal energy is around $\sqrt{s_{NN}}=3-5$ GeV, where a baryon density $\rho/\rho_0 = 3$ nuclear density is realized with a substantially large space-time volume. Higher and lower energies are disfavored due to short lifetime and low density

Multi-Purpose Detector (MPD) Collaboration



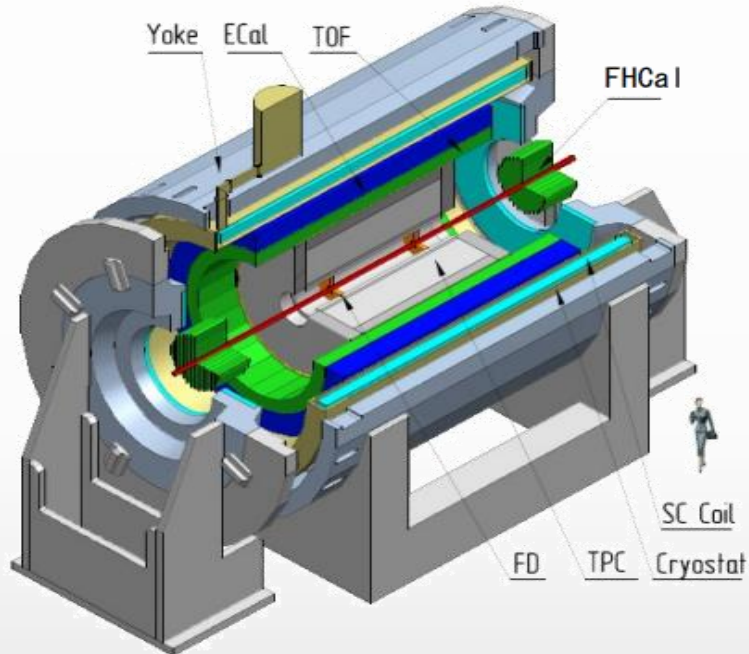
*MPD International Collaboration was established in 2018
to construct, commission and operate the detector*

10 Countries, >450 participants, 31 Institutes and JINR

Organization

Acting Spokesperson: **Victor Riabov**
Deputy Spokesperson: **Zebo Tang**
Institutional Board Chair: **Alejandro Ayala**
Project Manager: **Slava Golovatyuk**

Joint Institute for Nuclear Research;
AANL, Yerevan, **Armenia**;
University of Plovdiv, **Bulgaria**;
Tsinghua University, Beijing, **China**;
USTC, Hefei, **China**;
Huzhou University, Huizhou, **China**;
Institute of Nuclear and Applied Physics, CAS, Shanghai, **China**;
Central China Normal University, **China**;
Shandong University, Shandong, **China**;
IHEP, Beijing, **China**;
University of South China, **China**;
Three Gorges University, **China**;
Institute of Modern Physics of CAS, Lanzhou, **China**;
Tbilisi State University, Tbilisi, **Georgia**;
FCFM-BUAP (Heber Zepeda) Puebla, **Mexico**;
FC-UCOL (Maria Elena Tejeda), Colima, **Mexico**;
FCFM-UAS (Isabel Dominguez), Culiacán, **Mexico**;
ICN-UNAM (Alejandro Ayala), Mexico City, **Mexico**;
Institute of Applied Physics, Chisinev, **Moldova**;
Institute of Physics and Technology, **Mongolia**;



Belgorod National Research University, **Russia**;
INR RAS, Moscow, **Russia**;
MEPhI, Moscow, **Russia**;
Moscow Institute of Science and Technology, **Russia**;
North Osetian State University, **Russia**;
NRC Kurchatov Institute, ITEP, **Russia**;
Kurchatov Institute, Moscow, **Russia**;
St. Petersburg State University, **Russia**;
SINP, Moscow, **Russia**;
PNPI, Gatchina, **Russia**;
Vinča Institute of Nuclear Sciences, **Serbia**;
Pavol Jozef Šafárik University, Košice, **Slovakia**

